Title Page

Dual-Modified Liposome for Targeted and Enhanced Gene Delivery into Mice Brain

Bruna dos Santos Rodrigues, Sushant Lakkadwala, Takahisa Kanekiyo and Jagdish Singh

Department of Pharmaceutical Sciences, School of Pharmacy, College of Health Professions, North Dakota State University, Fargo, North Dakota 58105 (B.S.R.; S.L.; J.S.) and Department of Neuroscience, Mayo Clinic, Jacksonville, Florida 32224 (T.K.).

Running Title Page

Dual-Targeted Liposome for Gene Delivery to Mice Brain

Corresponding author: Jagdish Singh. Department of Pharmaceutical Sciences, School of Pharmacy, College of Health Professions, North Dakota State University, Fargo, ND 58105, USA. Tel: +1-701-231-7943. Fax: +1-701-231-8333.E-mail: jagdish.singh@ndsu.edu.

Number of text pages: 37

Number of tables:1

Number of figures: 9 (+ 4 supplemental)

Number of references: 81

Number of words in the Abstract: 205

Number of words in Introduction: 710

Number of words in Discussion: 1977

Non-standard Abbreviations

BBB: Blood brain barrier

CPP: Cell-penetrating peptide

DOPE: 1,2-dioleoyl-sn-glycero-3-phosphoethanolamine

DOTAP:1,2-dioleoyl-3-trimethylammonium-propane

FBS: Fetal bovine serum

H&E: Hematoxylin and eosin

kFGF: Kaposi Fibroblast Growth Factor

Mel: Melittin

MTT: (3-(4,5-Dimethylthiazol-2-yl)-2,5-Diphenyltetrazolium Bromide)

TEER: Transendothelial electrical resistance

Tf: Transferrin

TfR: Transferrin receptor

Abstract

The development of neuropharmaceutical gene delivery systems requires strategies to obtain efficient and effective brain targeting as well as blood brain barrier (BBB) permeability. A brain targeted gene delivery system based on transferrin and cell-penetrating peptide dual-functionalized liposome, CPP-Tf-liposome, was designed and investigated for crossing BBB and permeating into the brain. We selected three sequences of CPPs [Melittin, kaposi fibroblast growth factor (kFGF) and PasR8] and compared their ability to internalize into the cells and, subsequently, improve the transfection efficiency. Study of intracellular uptake indicated that liposomal penetration into bEnd.3, primary astrocytes and primary neurons occurred through multiple endocytosis pathways and surface modification with Tf and CPP enhanced the transfection efficiency of the nanoparticles. A co-culture *in vitro* BBB model reproducing the *in vivo* anatomophysiological complexity of the biological barrier was developed to characterize the penetrating properties of these designed liposomes. The dual-functionalized liposomes effectively transposed the *in vitro* barrier model followed by transfecting primary neurons. Liposome tissue distribution *in vivo* indicated superior ability of kFGFTf-liposomes to overcome BBB and reach brain of the mice after single IV administration. These findings demonstrate the feasibility of using strategically designed liposomes by combining Tf receptor targeting with enhanced cell penetration as a potential brain gene delivery vector.

Significance Statement

Rational synthesis of efficient brain-targeted gene carrier included modification of liposomes with a target-specific ligand, transferrin, and with cell-penetrating peptide to enhance cellular

internalization. Our study used an *in vitro* triple co-culture BBB model as a tool to characterize the permeability across BBB and functionality of designed liposomes prior *in vivo* biodistribution studies. Our study demonstrated that rational design and characterization of BBB permeability are efficient strategies for development of brain-target gene carriers.

Introduction

The potential of gene therapy to restore normal cellular functions has raised the interest for treatment of devastating diseases such as neurodegenerative diseases(Costantini *et al.*, 2000). Great efforts have been directed towards the development of gene vectors which are able to deliver therapeutic nucleic acids intracellularly in a specific and targeted manner. A wide range of different types of vectors, such as inorganic particles, peptide-based, lipid-based or polymer-based vectors, have been studied, however, their non-satisfactory gene transfer efficacy have limited their progression as brain-targeted gene delivery carriers (Cook *et al.*, 2015; MG *et al.*, 2015; Johnsen and Moos, 2016; Zhou *et al.*, 2018). Designed liposomes have featured as a suitable brain-targeted gene delivery vectors, demonstrating abilities to transfect brain cells efficiently in *in vivo* studies (Saffari *et al.*, 2016; Niu *et al.*, 2018). Rational engineering of liposomal nanoparticles have been developed to reduce the limitations of brain-targeted gene carriers and provide controlled release properties, prolonged systemic circulation, stimulus responsive properties and also capacity for endosomal escape (Yameen *et al.*, 2014; Kang *et al.*, 2018; Saeedi *et al.*, 2019). Hydrophilic chains on surface of nanoparticles own the ability to shield them from protein binding, minimizing their interactions during systemic circulation (opsonization). This steric barrier will prevent nanoparticles from macrophage recognition and

rapid clearance, and consequently, prolonging their circulation half-life (Li and Huang, 2010; Nag and Awasthi, 2013). The hydrophilic polymer poly (ethylene glycol) (PEG) has been widely used for improving the pharmacokinetics of a variety of nanoparticles (Maria Laura Immordino *et al.*, 2006). Furthermore, the increased interbilayer repulsion provided by PEG chains on liposome surface avoids nanoparticle aggregation, consequently improving their stability (Maria Laura Immordino *et al.*, 2006).

Cell-penetrating peptides (CPPs) are functional carrier peptides of less than 30 amino acids that infiltrate live cells, in a non-invasive manner, and facilitate the cellular uptake of a variety of bioactive molecules (De Figueiredo *et al.*, 2014; Ramsey and Flynn, 2015). Several CPPs have been successfully used for the delivery of exogenous molecules, including oligonucleotides and proteins, and conjugation of these peptides to liposomes have demonstrated ability to enhance liposome-mediated transfection in cell cultures and *in vivo* (Khalil *et al.*, 2006, 2007; Zhang *et al.*, 2006; Kim *et al.*, 2010). In this study, we compared the potential of three different CPPs to enhance the gene delivery properties of CPP coupled liposomes. Melittin (Mel) is a 26-long amino acid derived from bee venom and presents strong interaction with plasma membrane promoting its rearrangement with subsequent formation of transmembrane pores, which facilitate the transport of cargo into the cell (Lundquist *et al.*, 2008; Qian and Heller, 2015; Pino-Angeles and Lazaridis, 2018). Mel derivatives have shown to enhance intracellular delivery of therapeutic macromolecules (Kyung *et al.*, 2018). Hydrophobic sequences such as Kaposi fibroblast growth factor (kFGF) have been reported relevant for intracellular delivery of nucleic acids, providing stable non-covalent DNA complexation and protection against nucleases together with the ability to translocate across the lipid bilayer of plasma membrane (Lin *et al.*, 1995; Upadhya and Sangave, 2016; Bolhassani *et al.*, 2017). The addition of hydrophobic sequence FFLIPKG,

known as penetration accelerating sequence (Pas), to the arginine-rich peptide R8 formed the hybrid PasR8, revealed to improve not only the carrier abilities but also facilitated the escape from endocytic lysosomes (Takayama *et al.*, 2009, 2012).

Similar to most of pharmaceutical products, CPPs also face limitations, which cover short duration of action, entrapment in endocytic vesicles and poor tissue specificity (Kristensen *et al.*, 2016). Specific cellular targeting for delivery systems can be addressed by conjugating selective moieties on the surface of the nanoparticles (Zylberberg *et al.*, 2017). Studies focused on targeted-brain delivery have extensively explored transferrin receptor as a potential transporting route through blood brain barrier (BBB) (Johnsen and Moos, 2016). Here, we developed plasmid DNA (pDNA)-loaded liposomes bearing CPP and Tf ligands. We explored the properties of liposomal nanoparticulate system for targeted and enhanced gene delivery into brain parenchyma by comparing three different types of CPPs (Mel, kFGF and PasR8) abilities to improve transferrin receptor-targeted liposome delivery properties. In addition, we investigated the transport processes and mechanisms by which CPP-Tf-liposomes cross the *in vitro* BBB model and, subsequently, transfect primary neurons. Thus, this evaluation will provide an initial inference of *in vivo* efficacy of nanoparticles to translocate across the BBB as well as will allow to optimize the development of brain-targeted gene carriers.

Material and Methods

Synthesis of CPP- and Tf-coupled DSPE-PEG

JPET Fast Forward. Published on June 19, 2020 as DOI: 10.1124/jpet.119.264127
This article has not been copyedited and formatted. The final version may differ from this version.

CPP [Melittin- Mel (GIGAVLKVLTTGLPALISWIKRKRQQ), Kaposi fibroblast growth factor-kFGF (AAVALLPAVLLALLAP) and PasR8 (FFLIPKGRRRRRRRRGC); Ontores Biotechnologies, Hangzhou, Zhejiang, China] and holo-transferrin (Tf) (Sigma–Aldrich, St. Louis, MO, USA) were conjugated with terminal NHS-activated DSPE-PEG_{2000} (Biochempeg Scientific Inc., Watertown, MA, USA) through nucleophilic substitution reaction, separately. Briefly, CPP and DSPE-PEG_{2000}-NHS were mixed in anhydrous DMF at 1:5 molar ratio, and adjusted pH to 8.0-9.0 with triethylamine (Cai *et al.*, 2014; Layek *et al.*, 2014). After 120 h under moderate stirring at room temperature, the resulting reaction product was dialyzed (dialysis membrane with molecular weight cut off of 3500 Da) for 48 h.

Tf and DSPE-PEG_{2000}-NHS (125 µg of Tf/µM of DSPE-PEG_{2000}-NHS) were mixed in anhydrous DMF and adjusted pH to 8.0-9.0 with triethylamine (Li *et al.*, 2009; Sharma *et al.*, 2014; dos Santos Rodrigues, Banerjee, *et al.*, 2019). After 12 h of reaction, the mixture was dialyzed (dialysis membrane MWCO of 3500 Da) for 48 h.

Preparation of liposomal formulations

CPP-PEG-DSPE (4 mol %) along with DOPE-DOTAP-cholesterol (45:45:2 mol %, respectively) were used to prepare CPP-liposomes using thin lipid hydration method(Layek *et al.*, 2014; Sharma *et al.*, 2014; Liu *et al.*, 2017). PBS (pH 7.4) was used to hydrate the thin lipid film. Tf-micelles (4 mol %) was added to CPP-liposomes formed in the previous process and mixed overnight resulting in Tf-CPP-liposomes. Plasmid DNA was complexed to chitosan at N/P of 5 and then inserted into the liposomal formulations. Fluorescent-labeled liposomes were prepared by incorporating 1,2-dioleoyl-sn-glycero-3-phosphoethanolamine-N-

(lissaminerhodamine B sulfonyl; Avanti Polar Lipids, Alabaster, AL, USA) at 0.5 mol % to liposomes. The particle size and zeta potential of liposomal formulations were determined *via* dynamic light scattering using Zetasizer Nano ZS 90 (Malvern Instruments, Malvern, UK) at 25 °C. Morphology of liposomal formulation was observed by transmission electron microscopy (TEM, JEM-2100, JEOL). Hoechst 33342 (0.15 µg/ml) was used to determine the percent of encapsulated chitosan-pDNA complexes into liposomes and fluorescence intensity was measured using SpectraMax spectrophotometer (Molecular Devices, San Jose, CA, USA) at λ_{ex} 354 nm and λ_{em} 458 nm. Percent encapsulation was calculated as fluorescence signal Hoechst 33342 divided by the fluorescence following addition of 0.5% Triton X-100 (Layek *et al.*, 2014; Liu *et al.*, 2017).

Protection assay against nuclease degradation

Liposomal formulations (Mel-lip, MelTf-lip, kFGF-lip, kFGFTf-lip, PasR8-lip and PasR8Tf-liposomes) containing 1 µg pDNA were incubated in the presence of DNase I (1unit) for 1 h at 37 °C (Wang *et al.*, 2011). Then, 5 µl of EDTA (100 mM) were added to terminate the enzymatic reaction. Next, 20 µl of heparin (5 mg/mL) was added to the samples and incubated for 2 h at room temperature. The released pDNA samples were loaded on 0.8% (w/v) agarose gel stained with EtBr (0.5 µg/ml) and electrophoresed at 80V in 0.5 X Tris-acetate-EDTA (TAE, Bio-Rad, CA, USA) buffer for 80 min. Free pDNA in the absence or presence of DNase I served as negative control and positive control, respectively.

Cell culture and animals

All cell types were cultured at 37 °C in humidified cell culture incubator and 5% CO_2. The cell line bEnd.3 obtained from ATCC was cultured in DMEM growth media containing 10% v/v fetal bovine serum (FBS) and 1% v/v antibiotics. Primary astrocytes and primary neurons were obtained from brain of 1-day-old rats (Sumners and Fregly, 1989). After removing carefully meninges and vessels, the brains were mechanically and enzymatically (DMEM containing 0.25% trypsin and DNase I (8 µg/ml)) dissociated. Astrocytes obtained from the dissociated cells of brain were maintained in DMEM supplemented with 10% v/v FBS and 1% v/v antibiotics. Purity of astrocyte cultures was checked by immunostaining for glial fibrillary acidic protein (GFAP) antibody. Primary neurons were obtained by treating the dissociated cells with 10 µM cytosine arabinoside at day 3. Media was replaced after 48 h and cells were allowed to grow for further 10 days. Primary neurons were cultured in DMEM containing 10% v/v plasma-derived horse serum and 1% v/v antibiotics. Purity of neuronal cultures was checked by immunostaining for anti-MAP2 antibody.

All the procedures and handling of rats and mice were approved by Institutional Animal Care and Use Committee (IACUC) at North Dakota State University. Male/female Sprague-Dawley rats (Charles River Laboratories, Wilmington, MA, USA) and male/female C57BL/6 (Jackson Laboratories, Bar Harbor, ME, USA) were housed under standard conditions and free access to food and water.

Cytotoxicity assay

Cytotoxicity of Mel-lip, MelTf-lip, kFGF-lip, kFGFTf-lip, PasR8-lip and PasR8Tf-liposomes in bEnd.3, primary astrocytes and primary neurons was assessed by MTT assay (Sharma *et al.*, 2012). The cells were seeded on 96-well plates ($1x10_4$cells/well) 24 h before the experiment. Cells were exposed to liposomal formulations at different phospholipid concentrations (100, 200, 400 and 600 nM) for 4 h. Subsequently, cells were washed twice with PBS and cultured with fresh media for another 48 h. Then, 10 µl of MTT (5mg/ml) was added in each well. After 3 h of incubation at 37 °C, the resulting crystals were dissolved by DMSO (100µl) and absorbance was measured at 570 nm. Cells not exposed to liposomal formulations were used as control and cell viability was calculated and expressed as the percentage of the control.

Cellular internalization study

Fluorescent labeled-liposomes were used to investigate the internalization of liposomal nanoparticles into the cells. The cells (bEnd.3, primary astrocytes and primary neurons) were cultured on 24-well plate 24 h before the experiment. Lissamine rhodamine labeled-liposomes (100 nM) were incubated for predetermined times (0.1, 0.25, 0.5, 1 and 4 h). After incubation, suspended formulations were removed, and the cells were washed three times with PBS. Cell membrane was lysed with 0.5% v/v Triton X-100 and lissamine rhodamine was extracted in methanol. Fluorescence intensity was measured by fluorescence spectrometry at λ_{ex}553 nm and λ_{em}570 nm.

Internalization mechanisms

For investigation of mechanisms of internalization of liposomal formulations, the aforementioned cells were exposed to endocytosis inhibitors: sodium azide (10 mM), chlorpromazine (10 µg/ml), amiloride (100 µg/ml) and colchicine (50 µg/ml) for 30 min (dos Santos Rodrigues, Banerjee, *et al.*, 2019). Then, fluorescent labeled-liposomes (100 nM) were incubated for 4 h. Subsequently, media was removed, and cells were washed three times with PBS. Cell membranes were lysed with 0.5% v/v Triton X-100 and lissamine rhodamine extracted in methanol. Fluorescence intensity was measured by spectrofluorometric method (λ_{ex}553 nm and λ_{em} 570 nm).

In vitro transfection efficiency

Liposomal formulations (100 nM) encapsulating 1µg of chitosan-pDNA complexes were added to bEnd.3, primary astrocytes and primary neurons and incubated for 4 h (Sharma *et al.*, 2012). Subsequently, media was removed, cell were washed three times with PBS and incubated in fresh media for 48 h. Percent of cells expressing GFP was evaluated using flow cytometer (FACS analysis- Accuri C6, MI, USA). Quantification of β-galactosidase activity was performed using β-gal assay kit. Total protein levels were determined by BCA assay.

Blood compatibility study

The test was performed following the method previously described (dos Santos Rodrigues *et al.*, 2018a). Briefly, blood was withdrawn from Sprague-Dawley rats and washed 3 times with PBS (pH 7.4). Then, 500 µl of either different concentrations of liposomal formulations (31.25 – 1000

nM), or only PBS (negative control), or 1% Triton X-100 (positive control) were incubated with 1.5 x 10_7 erythrocytes (500 µl) for 1 h at 37 °C. After incubation, the samples were centrifuged (1500 rpm for 10 min) and released hemoglobin in the supernatant was measured as absorbance at 540 nm. Hemolysis percentage was calculated considering the absorbance in presence of Triton X-100 as 100%.

Transport of liposomes across the *in vitro* BBB model

The designed *in vitro* BBB model constituted of primary astrocytes (1.5x 10_4 cells/cm_2) cultured on the lower surface of membrane inserts and bEnd.3 cells (1.5x 10_4 cells/cm_2) cultured on upper surface of membrane inserts (Nakagawa *et al.*, 2009; Helms *et al.*, 2016). Transendothelial electrical resistance (TEER) was monitored using $EVOM_2$ (World Precision Instruments, FL, USA). After the development of tight contact among cells, fluorescent labeled-liposomes (100 nM) were added to the upper compartment and fluorescence intensity of liposomes in the basolateral compartment was quantified over a period of 8 h. TEER was measured before and after transport study to verify membrane integrity. Sodium-fluorescein (Na-F, MW: 376.275 g/mol) (100 µg/ml), a barrier integrity marker, was used to determine the permeability of the *in vitro* model and compared to the permeability of liposomal formulations.

Transfection efficiency of liposomes in the triple cell culture model

Liposomal formulations encapsulating 1 µg chitosan-pDNA complexes were added to the upper compartment of inserts placed in plates with primary neurons cultured on the bottom. Inserts

were removed and media were replaced for fresh media after 8 h and cells were incubated for 48 h. Percent of cells expressing GFP was evaluated by flow cytometry and fluorescence microscopy.

In vivo biodistribution and biocompatibility

Fluorescent labeled-liposomal formulations were administrated *via* tail vein of C57BL/6 mice at dose of ~15.2 μmoles/kg body weight (n=6) (Sharma *et al.*, 2013). Fluorescence intensity of lissamine rhodamine was analyzed after 24 h in the mice and individual organs using neutral infrared (NIR) imaging. Tissues were weighted, homogenized with PBS and the dye extracted with chloroform:methanol (2:1). Fluorescence intensity was measured using spectrophotometer at λ_{ex} 560 nm and λ_{em} 580 nm. Data were normalized with the negative control treated with saline only. Tissue characteristics and the possible morphological changes after treatment were analyzed in tissue sections with hematoxylin-eosin (H&E) staining.

Statistical analysis

The *in vitro* studies were performed in four independent experiments and all data were expressed as mean ± SD. Statistical significance were evaluated using one-way analysis of variance (ANOVA) followed by Tukey multiple comparison post-hoc test using the software GraphPad Prism version 5.0. P-values <0.05 were considered statistically significant. Six mice per *in vivo* experimental condition were used to provide statistically valid data.

Results

Characterization of liposomal formulations

Liposomal formulations were prepared according to our previously reporting method(dos Santos Rodrigues *et al.*, 2018a) and they were optimized to generate highly multivalent nanoparticles that could cross the BBB efficiently. We modified the surface of liposomes with Tf ligand for targeting the transferrin receptors, which are expressed on the surface of brain capillary endothelial cells, and a CPP to enhance cell penetration. The lipid vesicles were obtained with a mean size average of 153 nm. Incorporation of Tf on liposome surface led to not significant increase of particle size as compared to the particle size of CPP-modified liposomes. The zeta potential of liposomes was obtained in the range of 16-22 mV, as shown in the Table 1. The TEM image of dual-modified liposomes (kFGFTf-liposomes) showed the spherical morphology of nanoparticles (Figure 1a). Encapsulation efficiency of plasmid DNAs into liposomes was studied showing favorable plasmid encapsulation with more than 84% efficiency.

pDNA protection assay against nuclease degradation

The protective effect of liposomes on encapsulated pDNA against enzymatic degradation was evaluated incubating liposomal formulations in the presence of DNase I. Gel agarose electrophoresis (Figure 1b) confirmed the ability of the liposomes to preserve the encapsulated pDNA in the presence of DNase I, whereas the naked DNA was fully digested in the same experimental conditions (Figure 1b, lane b). There were no significant changes in the plasmid band encapsulated into liposomes (Figure 1b, lanes e-h) as compared to control (Figure 1b, lane

a), indicating that encapsulation of pDNA into liposomes protected them against enzymatic degradation.

Cytotoxicity of liposomal formulations

The effects of different concentrations (100, 200, 400 and 600 nM) of liposomal formulations on viability of bEnd.3 (Figure 2a), primary astrocytes (Figure 2b) and primary neurons (Figure 2c) after 4 h incubation were evaluated through MTT assay. The lowest concentration (100 nM) did not significantly affect the cell viability of the aforementioned cells, which was approximately 90%. Cell viability of the cells significantly ($p < 0.05$) reduced to 65% at 600 nM phospholipid concentration of kFGF-lip, kFGFTf-lip, PasR8-lip and PasR8Tf-lip. At 600 nM phospholipid concentration, Mel-lip and MelTf-lip demonstrated 57.8% of cell viabilities, which is significantly ($p < 0.05$) lesser as compared to kFGF-lip, kFGFTf-lip, PasR8-lip and PasR8Tf-lip at the same phospholipid concentration. Considering our findings,100 nM phospholipid concentration was used for further *in vitro* experiments due to lower cytotoxicity for all liposomal formulations.

Cellular internalization study

Evaluation of internalization of liposomal formulations into bEnd.3, primary astrocytes and primary neurons showed that uptake occurred in a time-dependent manner. The dual modified liposomal formulations demonstrated 68.6%, 66.8 % and 66.4% cellular uptake in bEnd.3 cells (Figure 3a), primary astrocytes (Figure 3b) and primary neurons (Figure 3c), respectively after 4

h. The investigation of the mechanisms involved in liposome internalization into the cells was performed using known endocytosis inhibitors for the main endocytosis pathways. The results showed the uptake of various liposomes in bEnd.3, primary astrocytes and primary neurons, after pretreatment with endocytosis inhibitors (Figure 3d, e and f). Using a fluorescently labeled-liposomes, we observed differences in the mechanism of liposomes uptake dependent on cell types (Supplemental Figure 1a, b and c). Moreover, we observed that the ATP depletion induced by the energy-dependent endocytosis inhibitor sodium azide pretreatment significantly decreased the uptake of all liposomal formulations in the tested cells. Mel-liposomes internalization in bEnd.3 cells and primary astrocytes occurred through multiple endocytosis mechanisms, without predominance of either clathrin-mediated endocytosis, caveolae-mediated endocytosis or macropinocytosis. While, the internalization into primary neurons preferentially occurred *via* caveolae-mediated endocytosis and direct translocation was also observed. Uptake of MelTf-liposomes in bEnd.3, primary astrocytes and primary neurons was driven by multiple endocytosis pathways without significant predominance of one pathway.

Clathrin-mediated endocytosis showed to be the main mechanism for kFGF-lip internalization into bEnd.3 cells, whereas macropinocytosis was that for primary astrocytes and primary neurons. Penetration of kFGFTf-lip into primary neurons occurred mainly through clathrin-mediated endocytosis, but there was no preferential route for kFGFTf-lip uptake for bEnd.3 cells and primary astrocytes. The results suggested that uptake of PasR8-lip and PasR8Tf-lip by the aforementioned cells employs energy-dependent pathways with the involvement of clathrin-mediated endocytosis, caveolae-mediated endocytosis and macropinocytosis.

Transfection efficiency

To verify the potential of CPPTf-liposomes as an efficient gene delivery nanoplatform for treatment of neurodegenerative diseases, plasmid GFP and plasmid βgal were chosen as model genes to evaluate the ability of liposomes to transfect cells. The capability of the formulations to transfect cells were compared to that of commercially available transfection agent Lipofectamine 3000. bEnd.3, primary astrocytes and primary neurons were treated with Lipofectamine 3000 or liposomal formulations containing chitosan-pGFP. After treatment, GFP-expression was quantified by flow cytometer (Figure 4a, b and c) as well as was observed using a fluorescence microscope (Figure 4d). While β-galactosidase activity was measured in bEnd.3, primary astrocytes and primary neurons using βgal assay kit (Supplemental Figure 2a, b and c). Liposomes modified with both Tf and CPP induced higher number of cells expressing GFP as compared to Lipofectamine 3000 and CPP-liposomes in all tested cells. Dual modified liposomes demonstrated significant ($p < 0.05$) increase in the number of GFP-expressing cells (33% in bEnd.3, 22.1% in primary astrocytes and 18% in primary neurons) as compared to Lipofectamine 3000 (10% in bEnd.3, 14% in primary astrocytes, 6.6% in primary neurons). Liposomes conjugated to Tf and CPP containing pβgal, similarly to those liposomes containing pGFP, induced higher β-galactosidase activity in the tested cells as compared to Lipofectamine 3000 and single modified liposomes.

Transfection in primary neurons after transport of liposomes across *in vitro* BBB model

The *in vitro* BBB model was developed co-culturing brain endothelial cells (bEnd.3 cells) on the upper surface of culture inserts, primary astrocytes seeded on the lower surface of the culture

insert and primary neurons on the bottom of the culture wells. The integrity of this BBB model was characterized by measuring the TEER and the paracellular transport of sodium fluorescein across the co-culture. Using fluorescently labelled-liposomes, we showed that liposome transport across the *in vitro* co-culture BBB model occurred over time (Figure 5a). CPP-Tf-liposomes showed superior ability to cross the *in vitro* BBB as compared to CPP-liposomes. After 8h, approximately 10.8% of MelTf-lip, kFGFTf-lip and PasR8Tf-liposomes crossed the *in vitro* BBB model. The permeability coefficients of the previously mentioned formulations were 3.7-fold higher as compared to that of Na-F (Figure 5b). Despite the significantly ($p < 0.05$) higher permeability of the liposomal formulations when compared to Na-F, the values of TEER strongly indicates that liposomes did not cause membrane disruption or cellular damage after transport investigation, therefore the integrity of the cellular barrier was maintained throughout the experiment (Figure 5c).

Thereafter, the ability of dual modified liposomes to transfect primary neurons after crossing the *in vitro* BBB model was assessed. MelTf-lip, kFGFTf-lip and PasR8Tf-liposomes were able to induce similar expression of GFP in primary neurons (Figure 6a), as observed in the fluorescent images of primary neurons expressing GFP after treatment with the aforementioned liposomes (Figure 6b, c and d, respectively).

Hemolytic potential

Hemolytic potential of liposomal formulations was investigated at different phospholipid concentration (31.25-1000 nM) on rat erythrocytes after 1 h of incubation at 37 °C, as shown in Figure 7. Similar hemolysis profile was observed for kFGF-lip, kFGFTf-lip, PasR8-lip and

JPET Fast Forward. Published on June 19, 2020 as DOI: 10.1124/jpet.119.264127
This article has not been copyedited and formatted. The final version may differ from this version.

PasR8Tf-liposomes. At the lowest phospholipid concentration (31.25 nM), 1.4% of hemolysis was observed, which gradually increased to 12.2% hemolysis at 1000 nM phospholipid concentration. Whereas Mel-lip and MelTf-lip at 31.25 μM phospholipid concentration showed approximately 1.9% of hemolysis. These liposomal formulations significantly ($p < 0.05$) increased hemolysis at 1000 nM phospholipid concentration to 15.6%. Biomaterials with hemolytic index below 2% are classified as non-hemolytic, while the ones within the range 2%-5% are classified as slight hemolytic and the ones above 5% are classified as hemolytic, according to ISO Standard Practice for Assessment of Hemolytic Properties of Materials (Committee F04 Medical and Surgical Materials and Devices, 2009). Therefore, liposomal formulations at low phospholipid concentration were considered non-hemolytic, which suggested to be appropriate for intravenous administration.

In vivo biodistribution

Accessing the brain is one of the major hurdles faced by therapeutic agents for the treatment of CNS diseases. Intravenous administration of liposomal formulations intends to maximize the targeted delivery and facilitate liposomes to bypass the BBB. Then, Mel-lip, MelTf-lip, kFGF-lip, kFGFTf-lip, PasR8-lip and PasR8Tf-liposomes were intravenously injected at a dose of 15.2 μmoles/kg body weight in C57BL/6 mice. The evaluation of brain transport efficiency as well as the distribution in liver, kidneys, lungs, heart, spleen and blood of fluorescently labelled CPPTf-liposomes was performed after 24 h following tail vein injection and expressed as percentage of the injected dose per gram of tissue (%ID/g). The designed liposomes were able to overcome the BBB and permeate into the brain of mice. As shown in Figure 8, 2.7%, 3.2%, 2.3%, 5.7%, 2.1%

and 3.7% ID/g in the brain were quantified for Mel-lip, MelTf-lip, kFGF-lip, kFGFTf-lip, PasR8-lip and PasR8Tf-liposomes, respectively. Highlighting kFGFTf-liposome showed significantly ($p < 0.05$) higher ability to translocate across the BBB and reach the brain parenchyma as compared to all liposomal formulations. Biodistribution analysis showed that liver was the major organ where liposomal formulations accumulated (average of 14.6% ID/g of tissue), (Supplemental Figure 3). We could observe levels of liposomal formulations between 4.8% to 10.4%ID/g of tissue for both kidneys and lungs. While 5.4% and 3.2% ID/g of tissue were the highest values calculate in heart and spleen, respectively, and 3.5%ID/ml of blood was the highest amount of liposomes quantified in the blood (Supplemental Figure 3). Figure 8 and Supplemental Figure 4 depicted the relative fluorescent intensity of the main organs (brain, liver, kidneys, lungs, heart and spleen) analyzed after 24 h of administration with the liposomal formulations.

H&E staining reflected the biocompatibility of liposomal formulations (Figure 9). The control group, animals administered with PBS, exhibited a healthy pattern with cellular integrity. In the treated group, animals administered with liposomal formulations, cellular damage or change in morphology was not observed. Signs of cytotoxicity including cell shrinkage, fragmentation, change in cell volume or signs of necrosis or inflammation were also not observed.

Discussion

Despite the advancement in therapeutic transport technology, nanoparticle formulations to treat brain diseases are still not available. Engineering liposomes based on control of composition and surface modification are being attempted to achieve targeted and delivery properties (Bunker *et*

al., 2016; Zylberberg *et al.*, 2017). Our group has demonstrated that the design of liposomal nanoparticles surface modified with Tf and cell-penetrating peptides results in efficient brain-targeted delivery systems (dos Santos Rodrigues *et al.*, 2018b; dos Santos Rodrigues, Kanekiyo, *et al.*, 2019; dos Santos Rodrigues, Lakkadwala, *et al.*, 2019; Lakkadwala *et al.*, 2019). Following the same concepts, we developed in this study liposomes modified with Tf and selected cell-penetrating peptides aiming to improve the delivery of plasmid DNA to brain cells after translocating the BBB. The transferrin receptors expressed on brain capillary endothelial cells help shuttle Tf-conjugated nanoparticles from blood into the brain, overcoming the impermeability of BBB. However, receptor saturation can interfere with the effects of Tf-nanoparticles and decrease their therapeutic efficacy (Johnsen and Moos, 2016; Gorain *et al.*, 2018). Therefore, these liposomes were surface modified with CPPs to overcome this effect.

Cell-penetrating peptides comprise a group of carriers with small peptide domains and the advantage of transporting cargo into the cells with no saturation phenomenon. In this study, we selected three CPPs (Mel, kFGF and PasR8) based on their physicochemical properties and reported ability to enhance the delivery properties of conjugated drug/gene carriers (Khanna *et al.*, 2015; Kyung *et al.*, 2018; Zhang *et al.*, 2018). We investigated the efficiency of liposomal nanoparticles modified with Tf and CPP as potential brain-targeted gene delivery systems.

Engineering our liposomal formulation included the lipid composition of nanoparticles, which consisted of DOTAP, DOPE, cholesterol and DSPE-PEG. The cationic character of DOTAP likely contributed to the overall positive zeta potential of liposomal formulations. The combination of DOTAP and the helper phospholipid DOPE has reported to cooperate with high transfection efficiency of such liposomal formulations (Hui *et al.*, 1996; Mochizuki *et al.*, 2013). These

phospholipids would facilitate the complexation with DNA and electrostatic interaction with plasma membrane followed by release of nucleic acid for successful transfection (Ciani *et al.*, 2004; Kim *et al.*, 2015). DOPE can additionally contribute to endosomal escape by destabilizing endosome membrane at low pH (Balazs and Godbey, 2009). Cholesterol incorporation intended to impart nanoparticle stability and control the release of genes (Briuglia *et al.*, 2015). While DSPE-PEG would improve pharmacokinetics of liposomes after intravenous administration by minimizing protein binding and recognition of the nanoparticles by reticuloendothelial systems (Maria Laura Immordino *et al.*, 2006). Complexation of plasmid DNA to chitosan was another strategy used in the design of liposomal gene delivery system with enhanced transfection efficiency. Chitosan, a cationic polymer, has extensive applications due to its versatile properties and safety. Gene delivery field has taken advantages of chitosan capacity to condense nucleic acids leading to protection against enzymatic degradation and promotion of transfection (Köping-Höggård *et al.*, 2001).

In this study, the designed brain-targeted liposomes were prepared using thin lipid film method followed by incorporation of Tf ligand through post-insertion method. The liposomal formulations showed homogeneous particle size which was supported by the narrow size distribution (PDI < 0.3). The presence of positively charged DOTAP and functional groups of Tf and CPPs may have contributed to the positive zeta potential of formulations.

Effective gene transfer is based on ensuring the delivery of the new genetic information into the target cells and the expression of the therapeutic molecule without disrupting essential regulatory functions (Ibraheem *et al.*, 2014). However, the hydrophilic anionic nature of DNA and their susceptibility to degradation by nucleases limit their passive penetration across plasma

membrane as well as their activity (Al-Dosari and Gao, 2009). Success of gene therapy depends on engineering a safe and effective carrier to ensure protection against nucleases and target delivery (Kumar *et al.*, 2016). Our designed liposomal formulations protected efficiently the encapsulated pDNA against nuclease degradation. Such protective properties were similar to those of surface modified liposomal formulations used in different studies (Lappalainen, 1994; Obata *et al.*, 2009; Meissner *et al.*, 2015).

Initially, the liposomal concentration used in our *in vitro* experiments was determined through evaluation of cytotoxicity in the target cells (brain endothelial cells, astrocytes and neurons). Corroborating with previous reports of our group with similar liposomal nanoparticles (dos Santos Rodrigues, Banerjee, *et al.*, 2019; dos Santos Rodrigues, Lakkadwala, *et al.*, 2019), the formulations had negligible cytotoxicity at low phospholipid concentration. However, cell viability significantly reduced at high phospholipid concentration, especially for Mel-conjugated liposomes. This can be due to the cell lytic capabilities of Mel. Supporting our findings, Mel has shown concentration and time-dependent cytotoxicity in studies with lymphocytes and such properties were associated to direct membrane toxicity as well as DNA damage (Pratt *et al.*, 2005; Lee *et al.*, 2007). Therefore, 100 nM phospholipid concentration was chosen for following experiments.

The better understanding of process that govern liposome interaction with cells, cellular internalization mechanisms and intracellular trafficking contribute to rational design and engineering of efficient gene delivery system (Behzadi *et al.*, 2017). The designed liposomes entered into bEnd.3, primary astrocytes and primary neurons in a time-dependent manner. Mechanistic understanding of the biological processes that determine the uptake of CPP coupled

liposomes as well as CPP and Tf coupled liposomes is important for further development of efficient gene delivery vectors with targeted properties, enhanced cellular internalization and efficient transfection. Liposome internalization into the cells begins with interaction of the liposome moieties to plasma membrane and subsequent activation of transport pathways (Veltman *et al.*, 2013; Behzadi *et al.*, 2017), which may occur either *via* endocytosis or direct translocation through plasma membrane. We were expecting that the selected liposome moieties should trigger the activation of endocytosis through sequence-specific interaction to cellular surface. Furthermore, we were also expecting differences in liposome uptake among the tested cells due to cell-to-cell variation in plasma membrane composition including proteoglycans and receptors, which consequently may influence intracellular destination of nanoparticles (Veltman *et al.*, 2013). Our results suggested that active endocytotic uptake mechanism was the major route for liposome internalization. The latter was in good accordance with findings on *in vitro* studies performed with cell-penetrating peptides (Ruzza *et al.*, 2010; Mo *et al.*, 2012) and surface modified-liposomes (Xu and Szoka, 1996; Bondurant *et al.*, 2002; Yamano *et al.*, 2011; Johnsen and Moos, 2016).

Mel-lip, MelTf-lip, PasR8-lipand PasR8Tf-lip internalized into the cells through multiple endocytosis pathways. While kFGF-lip preferentially internalized into bEnd.3 cells *via* clathrin-mediated endocytosis, and astrocytes and neurons *via* macropinocytosis. Clathrin-mediated endocytosis was the main mechanism for kFGFTf-lip internalize into primary neurons. The translocation potential of kFGF-conjugated cargos has been suggested to be related to the overall hydrophobic composition of the peptide (Khanna *et al.*, 2015). Our findings are in accordance with earlier reports showing that internalization of hydrophobic CPPs into cells happened mainly *via* endocytotic pathway (Gräslund *et al.*, 2011). Similarly, the promotion of PasR8 or peptide-

modified nanoparticles translocation into cytoplasm was observed to be predominantly an energy-dependent mechanism in different studies (Takayama *et al.*, 2009, 2012; Liu *et al.*, 2013). It suggested that mechanism was based on destabilization of plasma membrane during early stages of endocytosis. The hydrophobic segment Pas attached to R8 facilitated the peptide-proteoglycan interactions, thereby enhancing their internalization (Takayama *et al.*, 2009, 2012).

In vitro transfection studies showed that liposomal formulations dual-modified with Tf and CPP had superior ability to deliver pDNA into cells and induce higher protein expression when compared to CPP-liposomes and Lipofectamine. Our findings are in accordance with studies that demonstrated the enhancement in transfection provided by liposome modified with specific ligands (Zou *et al.*, 1999; Meissner *et al.*, 2015; Zylberberg *et al.*, 2017). Additionally, combination to transferrin-receptor targeting has consolidated to be a consistent strategy for both targeting properties and enhanced transfection (Cheng, 1996; Girão Da Cruz *et al.*, 2004; Girão da Cruz *et al.*, 2005).

A significant number of potential formulations for the treatment of CNS diseases fail to bypass the BBB. Therefore, it is relevant to characterize BBB permeability of these candidates in a reliable *in vitro* BBB model. This system can provide a better understating of mechanisms involved in crossing such tight barrier and can allow the screening as well as the optimization of candidate formulations (Hatherell *et al.*, 2011; Helms *et al.*, 2016). The designed co-culture BBB model provides close resemblance to the cell arrangement at the neurovasculature unit thereupon it has become a more widely accepted model (Wilhelm and Krizbai, 2014). Furthermore, the brain microvasculature cell line hCMEC/D3 represents an important human BBB model considering the expression of most transporters and receptors expressed in human BBB (Weksler

et al., 2013). In this study, we developed an *in vitro* BBB model consisting of mouse cells to mimic the brain vasculature of the animals used in the *in vivo* studies. In future studies, we would develop BBB model comprising of hCMEC/D3 cells for evaluating *in vitro* transport of liposomes. We would also use hCMEC/D3 cells to study cell uptake as well as transfection efficiency of liposomal formulations. The transport of liposomal formulations across the *in vitro* BBB occurred over time without disrupting the barrier layer, which correlates to the observed low cytotoxicity of liposomal formulations. Furthermore, the results suggest that transferrin receptor-targeting facilitated in interaction of CPPTf-liposomes to Tf receptor on cell surface enhancing the transport across the *in vitro* barrier layer. The translocation of Tf coupled liposomes suggested the involvement of clathrin-mediated transcytosis in this process.

Concerns about the biological safety of cationic nanoparticles administered intravenously need to be addressed prior *in vivo* application. The interaction between biomaterial and erythrocytes was evaluated using hemolysis assay. The hemolytic profile of liposomal formulations showed that hemolysis increased as phospholipid concentration increased. At low phospholipid concentration, hemolysis index was in the range classified as non-hemolytic (Committee F04 Medical and Surgical Materials and Devices, 2009). At higher phospholipid concentration, the superior levels of hemolysis induced by Mel-lip and MelTf-lip could be attributed due to the strong interaction of Mel to cell membranes, which can cause disruption of lipid structure accounting for erythrocytes lysis. Membrane binding and lysis properties of Mel depend not only on the plasma membrane composition, but also depend on peptide concentration (Lundquist *et al.*, 2008; Qian and Heller, 2015). Furthermore, conjugation to DSPE-PEG has demonstrated to reduce the lytic activity of Mel (Popplewell *et al.*, 2007). Taken together, these could be an explanation for the lower levels of hemolysis induced by Mel-lip and MelTf-lip at low

phospholipid concentration. The study of direct effects of Mel on erythrocytes exposed to Mel concentrations of 0.5 μM, 0.75 μM and 1μM demonstrated the lytic properties of this peptide, which produced variation on median cell volume followed by cell lysis (Pratt *et al.*, 2005). The low hemolytic index at low phospholipid concentration indicated that our designed liposomes are appropriate for systemic administration.

The qualitative and quantitative evaluation of biodistribution of our brain-targeted liposomes showed the ability of the nanoparticles to overcome the BBB and dual modification with both ligands enhanced the brain-targeting ability. Liposomes modified with kFGF and Tf showed significantly ($p<0.05$) higher accumulation in the brain compared to MelTf-lip and PasR8Tf-lip. Physicochemical properties of kFGF might have contributed to enhancement of transport of modified liposomes across BBB. The latter may be attributed to the reported high translocation across BBB with reduced efflux from the brain and longer half-life (~48 h) of kFGF compared to Mel and arginine-rich peptides (4 min and 2 h, respectively) (Sarko *et al.*, 2010; Khanna *et al.*, 2015). Additional studies are needed to investigate the mechanisms involved in nanoparticle transcytosis across BBB, delivery of pDNA and induction of protein expression in brain cells. Liposomal formulations were also detected in other organs and accumulated more in liver. Many research groups have developed advanced brain delivery carriers based on liposomes coated with specific ligands that ensure brain targeting and prolonged systemic circulation properties (Qin *et al.*, 2011; Zheng *et al.*, 2015; Gregori *et al.*, 2016; Ordóñez-Gutiérrez *et al.*, 2017; Gorain *et al.*, 2018). The brain targeted properties and accumulation of the designed liposomes combining transferrin-receptor targeting and enhanced cell penetration in our study showed advantageous application as brain gene carrier. Further, the overexpression of transferrin receptor on brain capillary endothelium could strength the targeting ability of dual-functionalized liposomes

JPET Fast Forward. Published on June 19, 2020 as DOI: 10.1124/jpet.119.264127
This article has not been copyedited and formatted. The final version may differ from this version.

especially of kFGFTf-liposomes. This finding followed the similar efficiency of liposomes to accumulate in the brain described in earlier reports of our group suggesting the importance of specific ligands enhancing the transport of multifunctionalized liposomes across BBB (dos Santos Rodrigues *et al.*, 2018b; dos Santos Rodrigues, Lakkadwala, *et al.*, 2019). Additionally, these studies also suggested that physicochemical properties of coupled CPPs determined the differences in the ability of liposomes to reach the brain. Studies characterizing the role of CPP on *in vivo* transport of designed liposomes across BBB may explain the differences in transport efficiency of formulations across the BBB and, consequently in transfection efficiency.

The biologically inspired lipid-based nanoparticles, conjugated to Tf ligand and CPP, were here designed as a novel nanomedicine for efficient delivery of genes into the brain. Both *in vitro* and *in vivo* experiments evaluated the ability of these liposomes to translocate across cell membrane and transfect cells. We could note that the physicochemical properties of the selected CPPs (Mel, kFGF and PasR8) influenced the ability of the designed liposomes to internalize and transfect cells as well as to cross *in vitro* and *in vivo* BBB and penetrate into the brain. The established *in vitro* co-culture BBB model showed to be a reliable model to estimate the ability of the delivery systems to penetrate into the central nervous system. Liposomes conjugated to Tf and kFGF showed significantly higher ability to overcome BBB and reach the brain of mice compared to the other dual-functionalized liposomes. The findings here provided evidence that strategic design of liposomal formulations might serve as efficient approach to obtain delivery system with desired properties. Importantly, the data also highlight the importance for strategic design of liposomal formulations involving the use of transferrin receptor-targeting and CPPs to improve carrier gene delivery properties prior to their translation *in vivo*.

Acknowledgment

B.S.R. is supported by doctoral fellowship from The Brazilian National Council for Scientific and Technological Development (CNPq, Brazil - Full Doctorate Fellowship (GDE): 221327/2014-2).

Authorship contributions

Participated in research design: Rodrigues, Lakkadwala, Kanekiyo, Singh.

Conducted experiments: Rodrigues.

Performed data analysis: Rodrigues.

Wrote and contributed to the writing of the manuscript: Rodrigues, Lakkadwala, Singh.

References

Al-Dosari MS, and Gao X (2009) Nonviral Gene Delivery: Principle, Limitations, and Recent Progress. *AAPS J* **11**:671–681.

Balazs DA, and Godbey WT (2009) Liposomes for Use in Gene Delivery. *Biomacromoles* **10**:2379–2400.

Behzadi S, Serpooshan V, Tao W, Hamaly MA, Alkawareek MY, Dreaden EC, Brown D, Alkilany AM, Farokhzad OC, and Mahmoudi M (2017) Cellular uptake of nanoparticles: Journey inside the cell. *Chem Soc Rev* **46**:4218–4244, Royal Society of Chemistry.

Bolhassani A, Jafarzade BS, and Mardani G (2017) In vitro and in vivo delivery of therapeutic proteins using cell penetrating peptides. *Peptides* **87**:50–63, Elsevier Inc.

Bondurant B, O'Brien DF, McLean SD, Miller CR, and McGovern KA (2002) Liposome−Cell Interactions in Vitro: Effect of Liposome Surface Charge on the Binding and Endocytosis of Conventional and Sterically Stabilized Liposomes † . *Biochemistry* **37**:12875–12883.

Briuglia M-L, Rotella C, McFarlane A, and Lamprou DA (2015) Influence of cholesterol on liposome stability and on in vitro drug release. *Drug Deliv Transl Res* **5**:231–242, Springer US.

Bunker A, Magarkar A, and Viitala T (2016) Rational design of liposomal drug delivery systems, a review: Combined experimental and computational studies of lipid membranes, liposomes and their PEGylation. *Biochim Biophys Acta - Biomembr* **1858**:2334–2352, Elsevier B.V.

Cai D, Gao W, He B, Dai W, Zhang H, Wang X, Wang J, Zhang X, and Zhang Q (2014) Hydrophobic penetrating peptide PFVYLI-modified stealth liposomes for doxorubicin delivery in breast cancer therapy. *Biomaterials* **35**:2283–2294, Elsevier Ltd.

Cheng P-W (1996) Receptor Ligand-Facilitated Gene Transfer: Enhancement of Liposome-Mediated Gene Transfer and Expression by Transferrin. *Hum Gene Ther* **7**:275–282, Mary Ann Liebert, Inc. 2 Madison Avenue Larchmont, NY 10538 USA.

Ciani L, Ristori S, Salvati A, Calamai L, and Martini G (2004) DOTAP/DOPE and DC-Chol/DOPE lipoplexes for gene delivery: Zeta potential measurements and electron spin resonance spectra. *Biochim Biophys Acta - Biomembr* **1664**:70–79.

Committee F04 Medical and Surgical Materials and Devices SF 1. BTM (2009) Standard practice for assessment of hemolytic properties of materials. *Annu B ASTM Stand* 1–5.

Cook RL, Householder KT, Chung EP, Prakapenka A V., Diperna DM, and Sirianni RW (2015) A critical evaluation of drug delivery from ligand modified nanoparticles: Confounding small molecule distribution and efficacy in the central nervous system. *J Control Release* **220**:89–97, Elsevier B.V.

Costantini LC, Bakowska JC, Breakefield XO, and Isacson O (2000) Gene therapy in the CNS. *Gene Ther* **7**:93–109, Nature Publishing Group.

De Figueiredo IR, Freire JM, Flores L, Veiga AS, and Castanho MARB (2014) Cell-penetrating peptides: A tool for effective delivery in gene-targeted therapies. *IUBMB Life* **66**:182–194.

dos Santos Rodrigues B, Banerjee A, Kanekiyo T, and Singh J (2019) Functionalized liposomal nanoparticles for efficient gene delivery system to neuronal cell transfection. *Int J Pharm* **566**:717–730, Elsevier.

dos Santos Rodrigues B, Kanekiyo T, and Singh J (2019) ApoE-2 Brain-Targeted Gene Therapy Through Transferrin and Penetratin Tagged Liposomal Nanoparticles. *Pharm Res* **36**:161.

dos Santos Rodrigues B, Lakkadwala S, Kanekiyo T, and Singh J (2019) Development and screening of brain-targeted lipid-based nanoparticles with enhanced cell penetration and gene delivery properties. *Int J Nanomedicine* **Volume 14**:6497–6517, Dove Press.

dos Santos Rodrigues B, Oue H, Banerjee A, Kanekiyo T, and Singh J (2018a) Dual functionalized liposome-mediated gene delivery across triple co-culture blood brain barrier model and specific in vivo neuronal transfection. *J Control Release* **286**:264–278, Elsevier.

dos Santos Rodrigues B, Oue H, Banerjee A, Kanekiyo T, and Singh J (2018b) Dual functionalized liposome-mediated gene delivery across triple co-culture blood brain barrier model and specific in vivo neuronal transfection. *J Control Release* **286**:264–278, Elsevier.

Girão da Cruz MT, Cardoso ALC, de Almeida LP, Simões S, and Pedroso de Lima MC (2005) Tf-lipoplex-mediated NGF gene transfer to the CNS: Neuronal protection and recovery in an excitotoxic model of brain injury. *Gene Ther* **12**:1242–1252.

Girão Da Cruz MT, Simões S, and Pedroso De Lima MC (2004) Improving lipoplex-mediated gene transfer into C6 glioma cells and primary neurons. *Exp Neurol* **187**:65–75.

Gorain B, Kesharwani P, Cheah JY, Chin PX, Phang YL, Hussain Z, Mak K-K, Choudhury H, Ooi SC, Pandey M, and Pichika MR (2018) Transferrin receptors-targeting nanocarriers for efficient targeted delivery and transcytosis of drugs into the brain tumors: a review of recent advancements and emerging trends. *Drug Deliv Transl Res* **8**:1545–1563, Drug Delivery and Translational Research.

Gräslund A, Madani F, Lindberg S, Langel Ü, and Futaki S (2011) Mechanisms of cellular uptake of cell-penetrating peptides. *J Biophys* **2011**.

Gregori M, Taylor M, Salvati E, Re F, Mancini S, Balducci C, Forloni G, Zambelli V, Sesana S, Michael M, Michail C, Tinker-Mill C, Kolosov O, Scherer M, Harris S, Fullwood NJ, Masserini M, and Allsop D (2016) Retro-inverso peptide inhibitor nanoparticles as potent inhibitors of aggregation of the Alzheimer's Aβ peptide. *Nanomedicine Nanotechnology, Biol Med* 1–10, Elsevier B.V.

Hatherell K, Couraud PO, Romero IA, Weksler B, and Pilkington GJ (2011) Development of a

three-dimensional, all-human in vitro model of the blood-brain barrier using mono-, co-, and tri-cultivation Transwell models. *J Neurosci Methods* **199**:223–229, Elsevier B.V.

Helms HC, Abbott NJ, Burek M, Cecchelli R, Couraud P-O, Deli MA, Förster C, Galla HJ, Romero IA, Shusta E V, Stebbins MJ, Vandenhaute E, Weksler B, and Brodin B (2016) In vitro models of the blood–brain barrier: An overview of commonly used brain endothelial cell culture models and guidelines for their use. *J Cereb Blood Flow Metab* **36**:862–890.

Hui SW, Langner M, Zhao YL, Ross P, Hurley E, and Chan K (1996) The role of helper lipids in cationic liposome-mediated gene transfer. *Biophys J* **71**:590–599.

Ibraheem D, Elaissari A, and Fessi H (2014) Gene therapy and DNA delivery systems. *Int J Pharm* **459**:70–83, Elsevier B.V.

Johnsen KB, and Moos T (2016) Revisiting nanoparticle technology for blood-brain barrier transport: Unfolding at the endothelial gate improves the fate of transferrin receptor-targeted liposomes. *J Control Release* **222**:32–46, Elsevier B.V.

Kang YJ, Cutler EG, and Cho H (2018) Therapeutic nanoplatforms and delivery strategies for neurological disorders. *Nano Converg* **5**, Springer Singapore.

Khalil IA, Kogure K, Futaki S, Hama S, Akita H, Ueno M, Kishida H, Kudoh M, Mishina Y, Kataoka K, Yamada M, and Harashima H (2007) Octaarginine-modified multifunctional envelope-type nanoparticles for gene delivery. *Gene Ther* **14**:682–689.

Khalil IA, Kogure K, Futaki S, and Harashima H (2006) High density of octaarginine stimulates macropinocytosis leading to efficient intracellular trafficking for gene expression. *J Biol*

Chem **281**:3544–3551.

Khanna M, Moutal A, FranÃ§ois-Moutal L, Khanna R, and Brittain JM (2015) Differential neuroprotective potential of CRMP2 peptide aptamers conjugated to cationic, hydrophobic, and amphipathic cell penetrating peptides. *Front Cell Neurosci* **8**:1–15.

Kim BK, Hwang GB, Seu YB, Choi JS, Jin KS, and Doh KO (2015) DOTAP/DOPE ratio and cell type determine transfection efficiency with DOTAP-liposomes. *Biochim Biophys Acta - Biomembr* **1848**:1996–2001, Elsevier B.V.

Kim HK, Davaa E, Myung CS, and Park JS (2010) Enhanced siRNA delivery using cationic liposomes with new polyarginine-conjugated PEG-lipid. *Int J Pharm* **392**:141–147, Elsevier B.V.

Köping-Höggård M, Tubulekas I, Guan H, Edwards K, Nilsson M, Vårum KM, and Artursson P (2001) Chitosan as a nonviral gene delivery system. Structure-property relationships and characteristics compared with polyethylenimine in vitro and after lung administration in vivo. *Gene Ther* **8**:1108–1121.

Kristensen M, Birch D, and Nielsen HM (2016) Applications and challenges for use of cell-penetrating peptides as delivery vectors for peptide and protein cargos. *Int J Mol Sci* **17**.

Kumar SR, Markusic DM, Biswas M, High KA, and Herzog RW (2016) Clinical development of gene therapy: results and lessons from recent successes. *Mol Ther - Methods Clin Dev* **3**:16034, Official journal of the American Society of Gene & Cell Therapy.

Kyung H, Kim H, Lee H, and Lee SJ (2018) Enhanced intracellular delivery of macromolecules by melittin derivatives mediated cellular uptake. *J Ind Eng Chem* **58**:290–295, The Korean

Society of Industrial and Engineering Chemistry.

Lakkadwala S, dos Santos Rodrigues B, Sun C, and Singh J (2019) Dual functionalized liposomes for efficient co-delivery of anti-cancer chemotherapeutics for the treatment of glioblastoma. *J Control Release* **307**:247–260, Elsevier.

Lappalainen K (1994) Biophysica Cationic liposomes improve stability and intracellular delivery of. **1196**:201–208.

Layek B, Haldar MK, Sharma G, Lipp L, Mallik S, and Singh J (2014) Hexanoic acid and polyethylene glycol double grafted amphiphilic chitosan for enhanced gene delivery: Influence of hydrophobic and hydrophilic substitution degree. *Mol Pharm* **11**:982–994.

Lee YJ, Kang SJ, Kim BM, Kim YJ, Woo HD, and Chung HW (2007) Cytotoxicity of honeybee (Apis mellifera) venom in normal human lymphocytes and HL-60 cells. *Chem Biol Interact* **169**:189–197.

Li SD, and Huang L (2010) Stealth nanoparticles: High density but sheddable PEG is a key for tumor targeting. *J Control Release* **145**:178–181, Elsevier B.V.

Li X, Ding L, Xu Y, Wang Y, and Ping Q (2009) Targeted delivery of doxorubicin using stealth liposomes modified with transferrin. *Int J Pharm* **373**:116–23.

Lin YZ, Yao S, Veach RA, Torgerson TR, and Hawiger J (1995) Inhibition of nuclear translocation of transcription factor NF-??B by a synthetic peptide containing a cell membrane-permeable motif and nuclear localization sequence.

Liu BR, Lo SY, Liu CC, Chyan CL, Huang YW, Aronstam RS, and Lee HJ (2013) Endocytic Trafficking of Nanoparticles Delivered by Cell-penetrating Peptides Comprised of Nona-

arginine and a Penetration Accelerating Sequence. *PLoS One* **8**:1–12.

Liu C, Liu XN, Wang GL, Hei Y, Meng S, Yang LF, Yuan L, and Xie Y (2017) A dual-mediated liposomal drug delivery system targeting the brain: Rational construction, integrity evaluation across the blood–brain barrier, and the transporting mechanism to glioma cells. *Int J Nanomedicine* **12**:2407–2425.

Lundquist A, Wessman P, Rennie AR, and Edwards K (2008) Melittin-Lipid interaction: A comparative study using liposomes, micelles and bilayerdisks. *Biochim Biophys Acta - Biomembr* **1778**:2210–2216.

Maria Laura Immordino, Franco Dosio, and Luigi Cattel (2006) Stealth liposomes: review of the basic science, rationale, and clinical applications, existing and potential. *Int J Nanomedicine* **1**:297–315.

Meissner JM, Toporkiewicz M, Czogalla A, Matusewicz L, Kuliczkowski K, and Sikorski AF (2015) Novel antisense therapeutics delivery systems: In vitro and in vivo studies of liposomes targeted with anti-CD20 antibody. *J Control Release* **220**:515–528, The Authors.

MG K, V K, and F H (2015) History and Possible Uses of Nanomedicine Based on Nanoparticles and Nanotechnological Progress. *J Nanomed Nanotechnol* **06**.

Mo RH, Zaro JL, and Shen WC (2012) Comparison of cationic and amphipathic cell penetrating peptides for siRNA delivery and efficacy. *Mol Pharm* **9**:299–309.

Mochizuki S, Kanegae N, Nishina K, Kamikawa Y, Koiwai K, Masunaga H, and Sakurai K (2013) The role of the helper lipid dioleoylphosphatidylethanolamine (DOPE) for DNA transfection cooperating with a cationic lipid bearing ethylenediamine. *Biochim Biophys*

Acta - Biomembr **1828**:412–418, Elsevier B.V.

Nag OK, and Awasthi V (2013) Surface engineering of liposomes for stealth behavior.

Nakagawa S, Deli MA, Kawaguchi H, Shimizudani T, Shimono T, Kittel Á, Tanaka K, and Niwa M (2009) A new blood-brain barrier model using primary rat brain endothelial cells, pericytes and astrocytes. *Neurochem Int* **54**:253–263.

Niu X, Chen J, and Gao J (2018) Nanocarriers as a powerful vehicle to overcome blood-brain barrier in treating neurodegenerative diseases: Focus on recent advances. *Asian J Pharm Sci* **14**:480–496, Elsevier B.V.

Obata Y, Saito S, Takeda N, and Takeoka S (2009) Plasmid DNA-encapsulating liposomes: Effect of a spacer between the cationic head group and hydrophobic moieties of the lipids on gene expression efficiency. *Biochim Biophys Acta - Biomembr* **1788**:1148–1158, Elsevier B.V.

Ordóñez-Gutiérrez L, Posado-Fernández A, Ahmadvand D, Lettiero B, Wu L, Antón M, Flores O, Moghimi SM, and Wandosell F (2017) ImmunoPEGliposome-mediated reduction of blood and brain amyloid levels in a mouse model of Alzheimer's disease is restricted to aged animals. *Biomaterials* **112**.

Pino-Angeles A, and Lazaridis T (2018) Effects of Peptide Charge, Orientation, and Concentration on Melittin Transmembrane Pores. *Biophys J* **114**:2865–2874, Biophysical Society.

Popplewell JF, Swann MJ, Freeman NJ, McDonnell C, and Ford RC (2007) Quantifying the effects of melittin on liposomes. *Biochim Biophys Acta - Biomembr* **1768**:13–20.

Pratt JP, Ravnic DJ, Huss HT, Jiang X, Orozc BS, and Mentzer SJ (2005) MELITTIN-INDUCED MEMBRANE PERMEABILITY : A NONOSMOTIC MECHANISM OF CELL DEATH To whom correspondence should be addressed at Brigham and Women ' s. 349–355.

Qian S, and Heller WT (2015) Melittin-induced cholesterol reorganization in lipid bilayer membranes. *Biochim Biophys Acta - Biomembr* **1848**:2253–2260, Elsevier B.V.

Qin Y, Chen H, Zhang Qianyu, Wang X, Yuan W, Kuai R, Tang J, Zhang L, Zhang Z, Zhang Qiang, Liu J, and He Q (2011) Liposome formulated with TAT-modified cholesterol for improving brain delivery and therapeutic efficacy on brain glioma in animals. *Int J Pharm* **420**:304–312, Elsevier B.V.

Ramsey JD, and Flynn NH (2015) Cell-penetrating peptides transport therapeutics into cells. *Pharmacol Ther* **154**:78–86, Elsevier Inc.

Ruzza P, Biondi B, Marchiani A, Antolini N, and Calderan A (2010) Cell-penetrating peptides: A comparative study on lipid affinity and cargo delivery properties. *Pharmaceuticals* **3**:1045–1062.

Saeedi M, Eslamifar M, Khezri K, and Dizaj SM (2019) Applications of nanotechnology in drug delivery to the central nervous system. *Biomed Pharmacother* **111**:666–675, Elsevier.

Saffari M, Moghimi HR, and Dass CR (2016) Barriers to liposomal gene delivery: From application site to the target. *Iran J Pharm Res* **15**:3–17.

Sarko D, Beijer B, Boy RG, Nothelfer EM, Leotta K, Eisenhut M, Altmann A, Haberkorn U, and Mier W (2010) The pharmacokinetics of cell-penetrating peptides. *Mol Pharm* **7**:2224–

2231, American Chemical Society.

Sharma G, Modgil A, Layek B, Arora K, Sun C, Law B, and Singh J (2013) Cell penetrating peptide tethered bi-ligand liposomes for delivery to brain in vivo: Biodistribution and transfection. *J Control Release* **167**:1–10, Elsevier B.V.

Sharma G, Modgil A, Sun C, and Singh J (2012) Grafting of cell-penetrating peptide to receptor-targeted liposomes improves their transfection efficiency and transport across blood-brain barrier model. *J Pharm Sci* **101**:2468–78.

Sharma G, Modgil A, Zhong T, Sun C, and Singh J (2014) Influence of short-chain cell-penetrating peptides on transport of doxorubicin encapsulating receptor-targeted liposomes across brain endothelial barrier. *Pharm Res* **31**:1194–209.

Sumners C, and Fregly MJ (1989) Modulation of angiotensin II binding sites in neuronal cultures by mineralocorticoids. *Am J Physiol* **256**:C121–C129.

Takayama K, Hirose H, Tanaka G, Pujals S, Katayama S, Nakase I, and Futaki S (2012) Effect of the attachment of a penetration accelerating sequence and the influence of hydrophobicity on octaarginine-mediated intracellular delivery. *Mol Pharm* **9**:1222–1230.

Takayama K, Nakase I, Michiue H, Takeuchi T, Tomizawa K, Matsui H, and Futaki S (2009) Enhanced intracellular delivery using arginine-rich peptides by the addition of penetration accelerating sequences (Pas). *J Control Release* **138**:128–133, Elsevier B.V.

Upadhya A, and Sangave PC (2016) Hydrophobic and electrostatic interactions between cell penetrating peptides and plasmid DNA are important for stable non-covalent complexation and intracellular delivery. *J Pept Sci* **2**:647–659.

Veltman K, Hendriks AJ, van Wezel A, Kettler K, and van de Meent D (2013) Cellular uptake of nanoparticles as determined by particle properties, experimental conditions, and cell type. *Environ Toxicol Chem* **33**:481–492.

Wang B, He C, Tang C, and Yin C (2011) Effects of hydrophobic and hydrophilic modifications on gene delivery of amphiphilic chitosan based nanocarriers. *Biomaterials* **32**:4630–4638, Elsevier.

Wilhelm I, and Krizbai IA (2014) In vitro models of the blood-brain barrier for the study of drug delivery to the brain. *Mol Pharm* **11**:1949–1963.

Xu Y, and Szoka FC (1996) Mechanism of DNA release from cationic liposome/DNA complexes used in cell transfection. *Biochemistry* **35**:5616–5623.

Yamano S, Dai J, Yuvienco C, Khapli S, Moursi AM, and Montclare JK (2011) Modified Tat peptide with cationic lipids enhances gene transfection efficiency via temperature-dependent and caveolae-mediated endocytosis. *J Control Release* **152**:278–285, Elsevier B.V.

Yameen B, Choi W Il, Vilos C, Swami A, Shi J, and Farokhzad OC (2014) Insight into nanoparticle cellular uptake and intracellular targeting. *J Control Release* **190**:485–499, Elsevier B.V.

Zhang C, Tang N, Liu XJ, Liang W, Xu W, and Torchilin VP (2006) siRNA-containing liposomes modified with polyarginine effectively silence the targeted gene. *J Control Release* **112**:229–239.

Zhang Q, Wang J, Zhang H, Liu D, Ming L, Liu L, Dong Y, Jian B, and Cai D (2018) The

anticancer efficacy of paclitaxel liposomes modified with low-toxicity hydrophobic cell-penetrating peptides in breast cancer: An: in vitro and in vivo evaluation. *RSC Adv* **8**:24084–24093, Royal Society of Chemistry.

Zheng C, Ma C, Bai E, Yang K, and Xu R (2015) Transferrin and cell-penetrating peptide dual-functioned liposome for targeted drug delivery to glioma. *Int J Clin Exp Med* **8**:1658–1668.

Zhou Y, Peng Z, Seven ES, and Leblanc RM (2018) Crossing the blood-brain barrier with nanoparticles. *J Control Release* **270**:290–303, Elsevier.

Zou L, Huang L, Hayes R, Black C, Qiu Y, Perez-Polo J, Le W, Clifton G, and Yang K (1999) Liposome-mediated NGF gene transfection following neuronal injury: potential therapeutic applications. *Gene Ther* **6**:994–1005.

Zylberberg C, Gaskill K, Pasley S, and Matosevic S (2017) Engineering liposomal nanoparticles for targeted gene therapy. *Gene Ther* **24**:441–452, Nature Publishing Group.

Footnotes

This work was supported by National Institutes of Health (Grant R01AG051574).

Legend of Figures

Figure 1. **a)** Transmission electron micrograph (TEM) of kFGFTf-liposomes which was negatively stained with 0.1% phosphotungstic acid aqueous solution (Scale 50 nm). **b)** Protective effect of liposomal formulations containing chitosan-pDNA complexes against nuclease degradation. Liposomal formulation containing chitosan-pGFP (N/P 5). Lane a, naked pGFP; lane b, naked pGFP+DNase I; lanes c-h, Mel-lip, MelTf-lip, kFGF-lip, kFGFTf-lip, PasR8-lip and PasR8Tf-liposomes containing chitosan-GFP complexes, respectively + DNase I.

Figure 2. *In vitro* viability of (a) bEnd.3 cells, (b) primary astrocytes and (c) primary neurons treated with Mel-lip, MelTf-lip, kFGF-lip, kFGFTf-lip, PasR8-lip and PasR8Tf-liposomes at different phospholipid concentrations (100, 200, 400 and 600 nM) for 4 h. Cell viability was determined by MTT assay. Data are expressed as mean ± SD (n=4). Statistically significant ($p<0.05$) differences are shown as (*).

Figure 3. Cellular uptake of Mel-lip, MelTf-lip, kFGF-lip, kFGFTf-lip, PasR8-lip and PasR8Tf-liposomes. The amount of DiI labeled-liposomes incorporated into (a) bEnd.3, (b) primary astrocytes and (c) primary neurons was measured after 0.1, 0.25, 0.5, 1 and 4 h of incubation. Statistically significant ($p<0.05$) differences are shown as (***) as compared to liposome uptake after 4 h of incubation. The amount of DiI labeled-liposomes incorporated after 4 h of incubation into (d) bEnd.3, (e) primary astrocytes and (f) primary neurons pretreated with endocytosis inhibitors (sodium azide, chlorpromazine, amiloride and colchicine). All data are expressed as

mean ± SD (n=4). Statistically significant ($p<0.05$) differences are shown as (***) as compared to control group (4h of incubation without endocytosis inhibitors).

Figure 4. GFP expression in bEnd.3 (a), primary astrocytes (b) and primary neurons (c) after 48 h of treatment with Mel-lip, MelTf-lip, kFGF-lip, kFGFTf-lip, PasR8-lip and PasR8Tf-liposomes containing chitosan-pGFP complexes as determined by flow cytometry. d) Fluorescence microscopy images of GFP expression in bEnd.3, primary astrocytes and primary neurons transfected with Mel-lip, MelTf-lip, kFGF-lip, kFGFTf-lip, PasR8-lip and PasR8Tf-liposomes containing chitosan-pGFP complexes after 48 h (Scale bar depicts 100 μm). Data are expressed as mean ± SD (n=4). Statistically significant ($p<0.05$) differences are shown as (*) with Lipofectamine 3000.

Figure 5. a) Percent transport of Non-modified liposome, Mel-lip, MelTf-lip, kFGF-lip, kGFGTf-lip, PasR8-lip and PasR8Tf-liposomes across *in vitro* BBB model over a period of 8 h. **b**) Endothelial cell permeability (Pe, expressed as $1x10^{-6}$ cm/sec) coefficient for Na-F, Non-modified, Mel-lip, MelTf-lip, kFGF-lip, KFGFTf-lip, PasR8-lip and PasR8Tf-liposomes. Statistically significant ($p<0.05$) difference is shown as (*) with Na-F. **c**) Transendothelial electrical resistance (TEER, expressed as Ωcm2) of *in vitro* BBB model before and after 8 h of incubation with liposomal formulations. All data are expressed as mean ± SD (n=4).

Figure 6. a) GFP expression in primary neurons transfected with MelTf-lip, kFGFTf-lip, and PasR8Tf-liposomes containing chitosan-GFP complexes after liposome transport through the *in vitro* BBB model as determined by flow cytometry. Fluorescence microscopy images of GFP

expression in primary neurons transfected with (**b**) MelTf-lip, (**c**) kFGFTf-lip and (**d**) PasR8Tf-liposomes containing chitosan-pGFP complexes after liposome transport study (Scale bar depicts 100 μm).

Figure 7. Hemolytic activity of Mel-lip, MelTf-lip, kFGF-lip, kFGFTf-lip, PasR8-lip and PassR8Tf-liposomes at different concentrations (31.25-1000 nM) in erythrocyte solution (2%) after 1 h of incubation at 37 °C. Hemolytic activity of 1% v/v Triton X-100 was considered as 100% hemolysis. Data are expressed as mean ± SD (n=4).

Figure 8. *In vivo* biodistribution and near-infrared (NIR) imaging of relative fluorescence intensity in the brain and whole mice after 24 h of Mel-lip, MelTf-lip, kFGF-lip, kFGFTf-lip, PasR8-lip and PasR8Tf-liposomes administration. Data are expressed as mean ± SE (n=6). Statistically significant ($p<0.05$) differences are shown as (*).

Figure 9. Representative images of hematoxylin-eosin (H&E) staining of brain, liver, kidneys, heart, lungs and spleen sections of C57BL/6 mice following tail vein administration of saline (used as control), Mel-lip, MelTf-lip, kFGF-lip, kFGFTf-lip, PasR8-lip and PasR8Tf-liposomes, n=6. Scale bar depicts 100 μm.

JPET Fast Forward. Published on June 19, 2020 as DOI: 10.1124/jpet.119.264127
This article has not been copyedited and formatted. The final version may differ from this version.

Table

Table 1: Characterization of CPPTf-liposomes

Liposomes	Size (nm)	PDI[a]	Zeta potential (mV)	EE[b]
Mel-liposome	150.9±3.39	0.287±0.02	20.9±2.58	87.4±3.85%
MelTf-liposome	165.5±3.52	0.175±0.05	19.9±1.63	84.6±4.89%
kFGF-liposome	145.9±4.18	0.237±0.04	16.3±0.81	84.5±1.97%
kFGFTf-liposome	151.5±3.47	0.192±0.03	20.1±1.21	90.7±1.96%
PasR8-liposome	147.3±2.46	0.274±0.05	21.3±1.13	88.2±7.40%
PasR8Tf-liposome	153.5±3.79	0.181±0.01	21.7±2.50	90.2±7.30%

Data are presented as mean ± SD from four different preparations.

[a]PDI: polydispersity index

[b]EE: pDNA entrapment efficiency

JPET Fast Forward. Published on June 19, 2020 as DOI: 10.1124/jpet.119.264127
This article has not been copyedited and formatted. The final version may differ from this version.

Figure 1

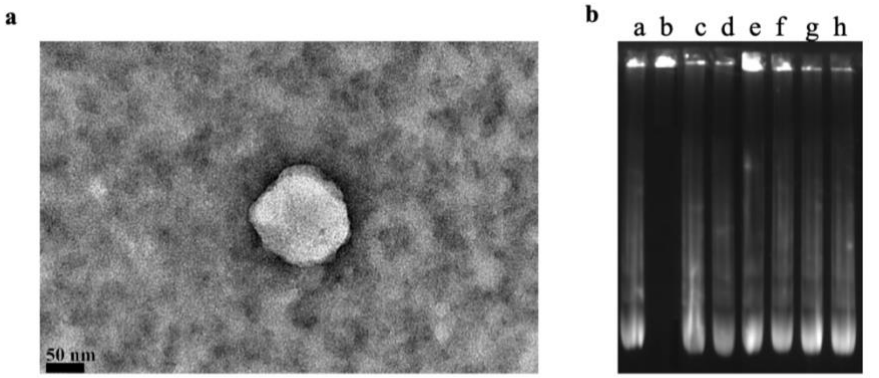

JPET Fast Forward. Published on June 19, 2020 as DOI: 10.1124/jpet.119.264127
This article has not been copyedited and formatted. The final version may differ from this version.

Figure 2

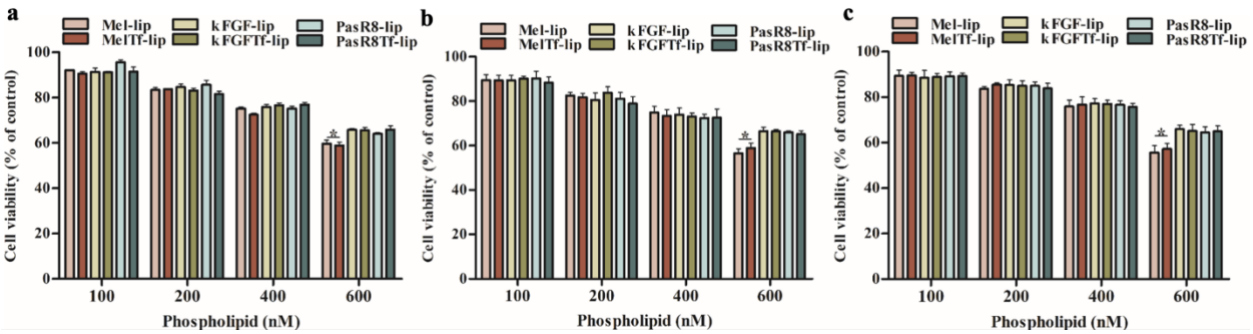

JPET Fast Forward. Published on June 19, 2020 as DOI: 10.1124/jpet.119.264127
This article has not been copyedited and formatted. The final version may differ from this version.

Figure 3

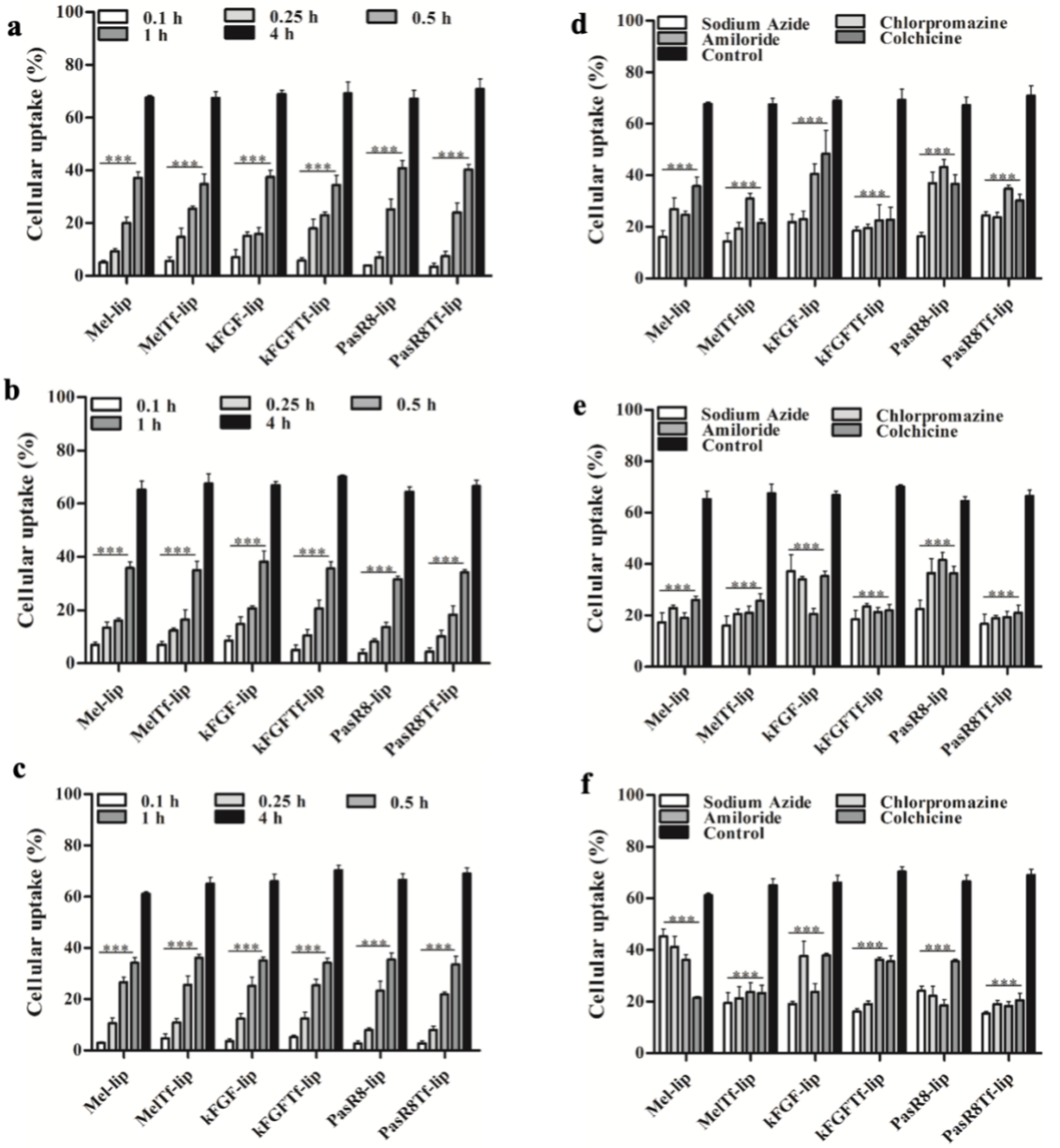

JPET Fast Forward. Published on June 19, 2020 as DOI: 10.1124/jpet.119.264127
This article has not been copyedited and formatted. The final version may differ from this version.

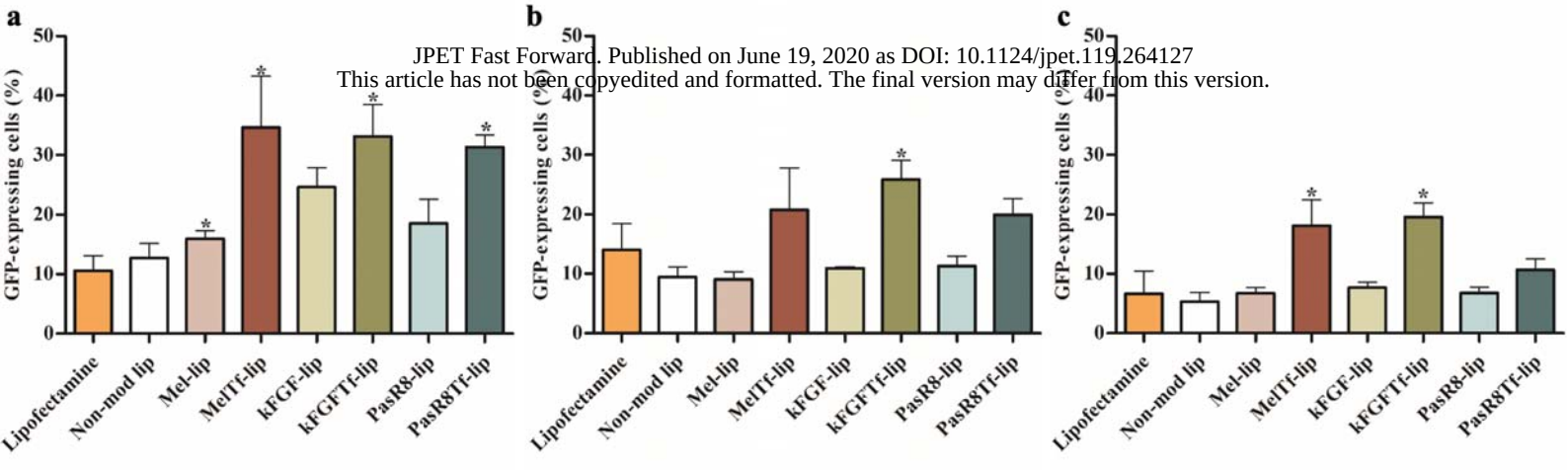

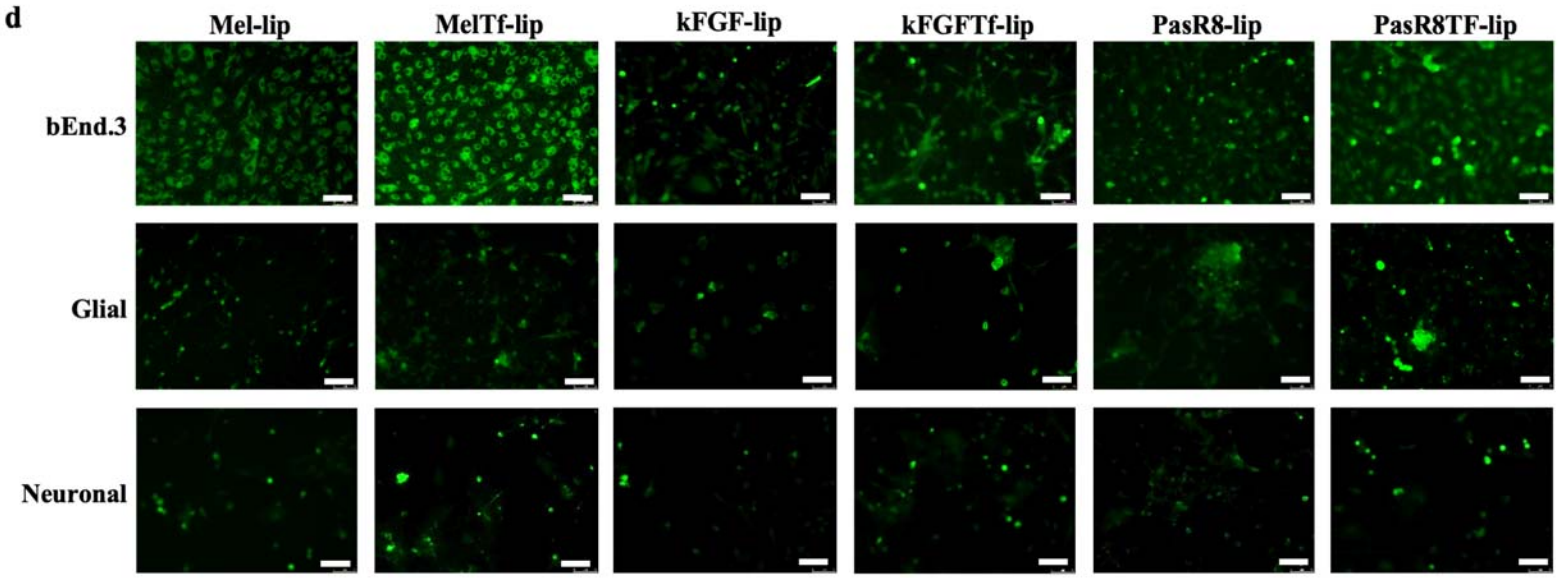

JPET Fast Forward. Published on June 19, 2020 as DOI: 10.1124/jpet.119.264127
This article has not been copyedited and formatted. The final version may differ from this version.

Figure 5

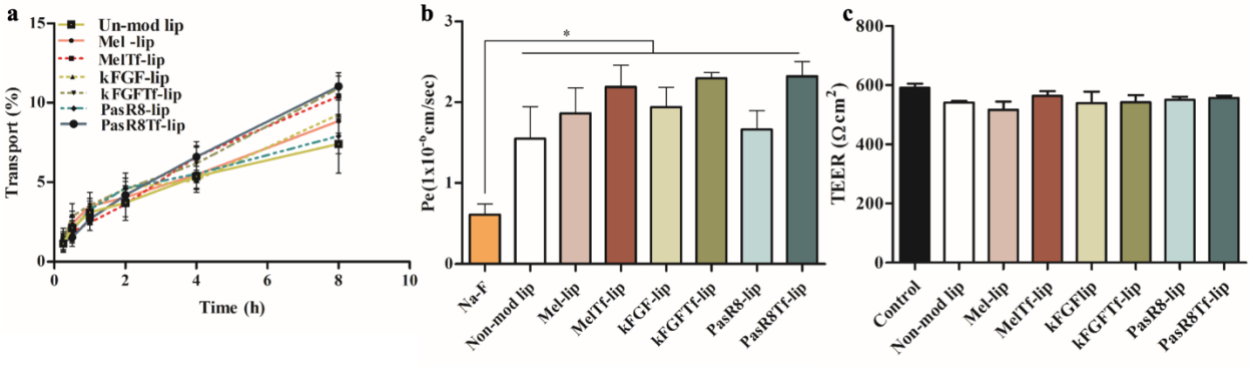

JPET Fast Forward. Published on June 19, 2020 as DOI: 10.1124/jpet.119.264127
This article has not been copyedited and formatted. The final version may differ from this version.

Figure 6

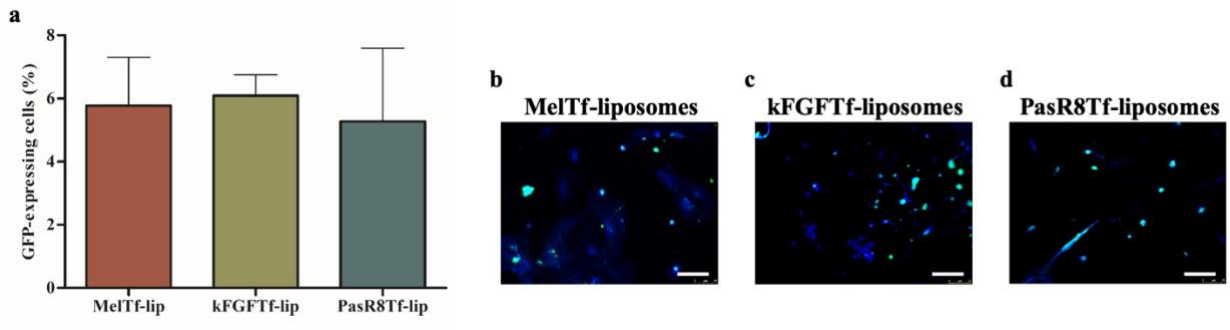

JPET Fast Forward. Published on June 19, 2020 as DOI: 10.1124/jpet.119.264127
This article has not been copyedited and formatted. The final version may differ from this version.

Figure 7

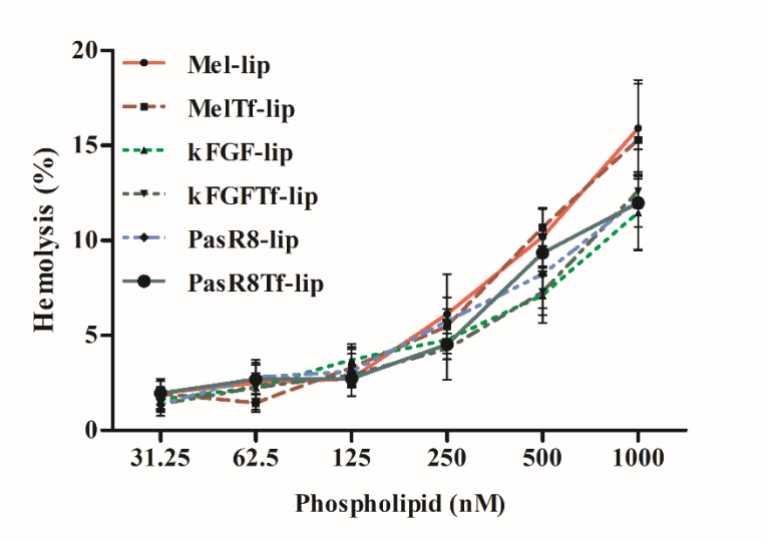

JPET Fast Forward. Published on June 19, 2020 as DOI: 10.1124/jpet.119.264127
This article has not been copyedited and formatted. The final version may differ from this version.

Figure 8

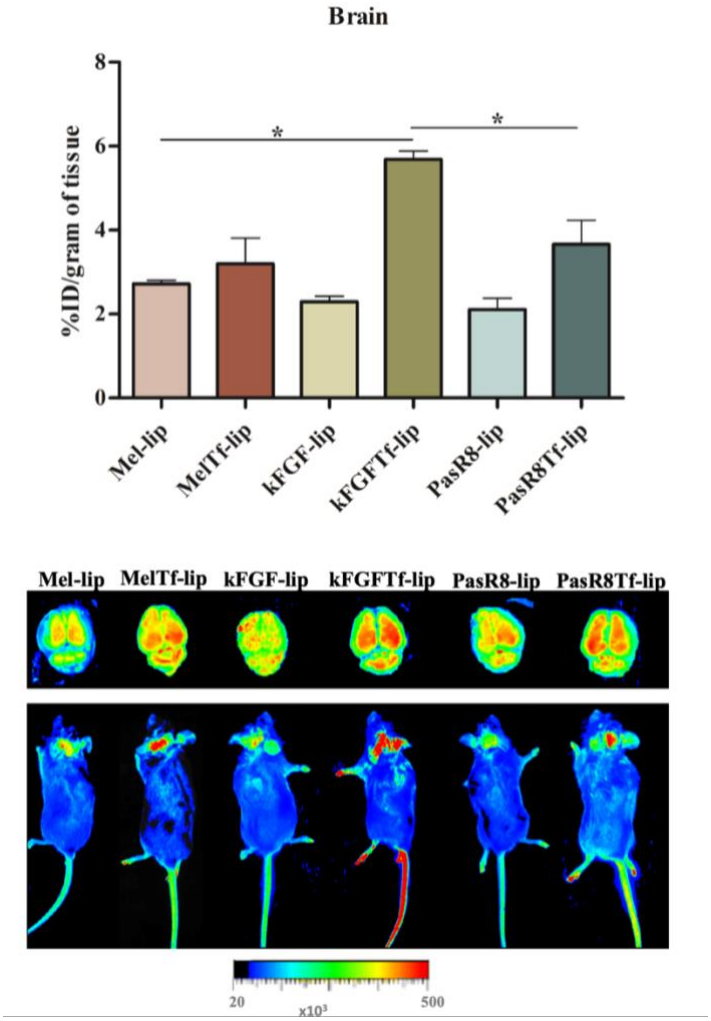

JPET Fast Forward. Published on June 19, 2020 as DOI: 10.1124/jpet.119.264127
This article has not been copyedited and formatted. The final version may differ from this version.

Figure 9

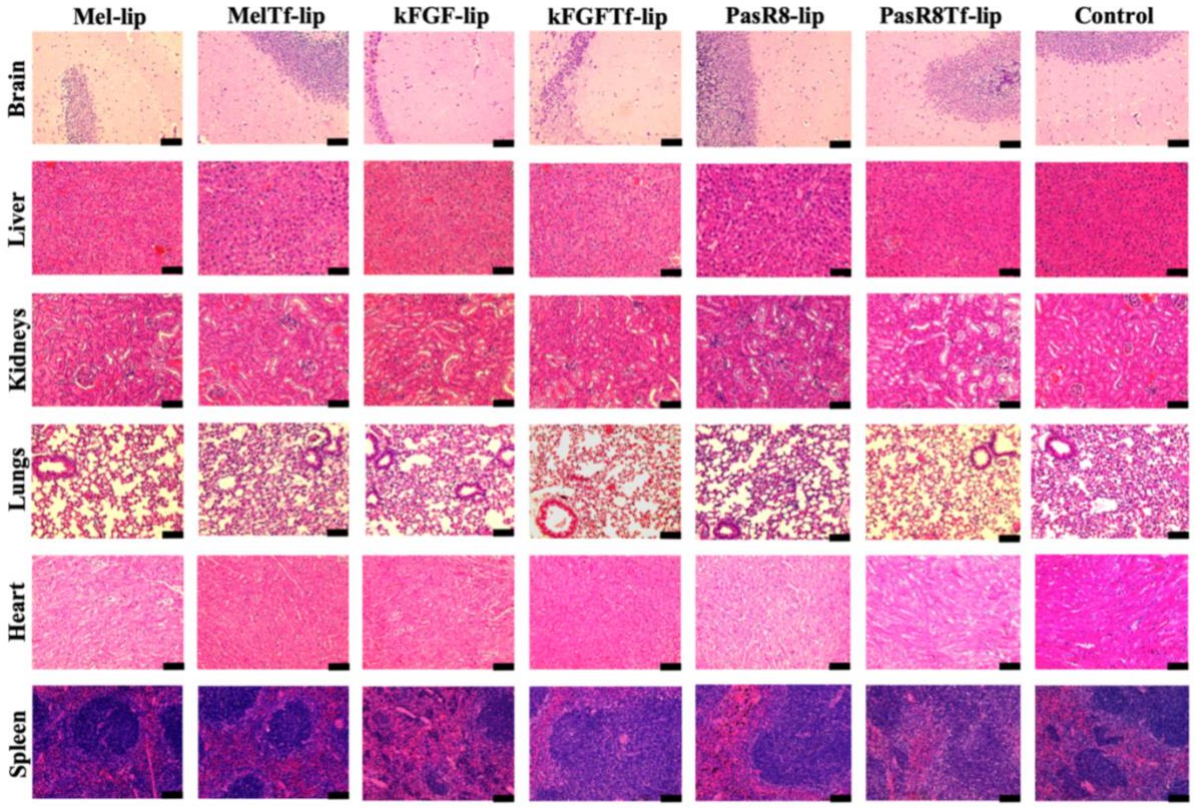

Journal of Pharmacology and Experimental Therapeutics

Supplemental data

Dual-Modified Liposome for Targeted and Enhanced Gene Delivery into Mice Brain

Bruna dos Santos Rodrigues, Sushant Lakkadwala, Takahisa Kanekiyo and Jagdish Singh

Supplemental Table 1: Participle size and encapsulation efficiency of kFGFTf-liposomes (380 nM phospholipid) containing different amount of pDNA-chitosan complexes

Characterization of liposomes	**kFGFTf-liposomes**	
	380 nM phospholipid + 25 µg pDNA complexed to chitosan (N/P=5)	380 nM phospholipid + 500 µg pDNA complexed to chitosan (N/P=5)
Particle size	153.1±3.72	154.3±1.35
Encapsulation Efficiency	91.3±5.54%	89.5±0,91%

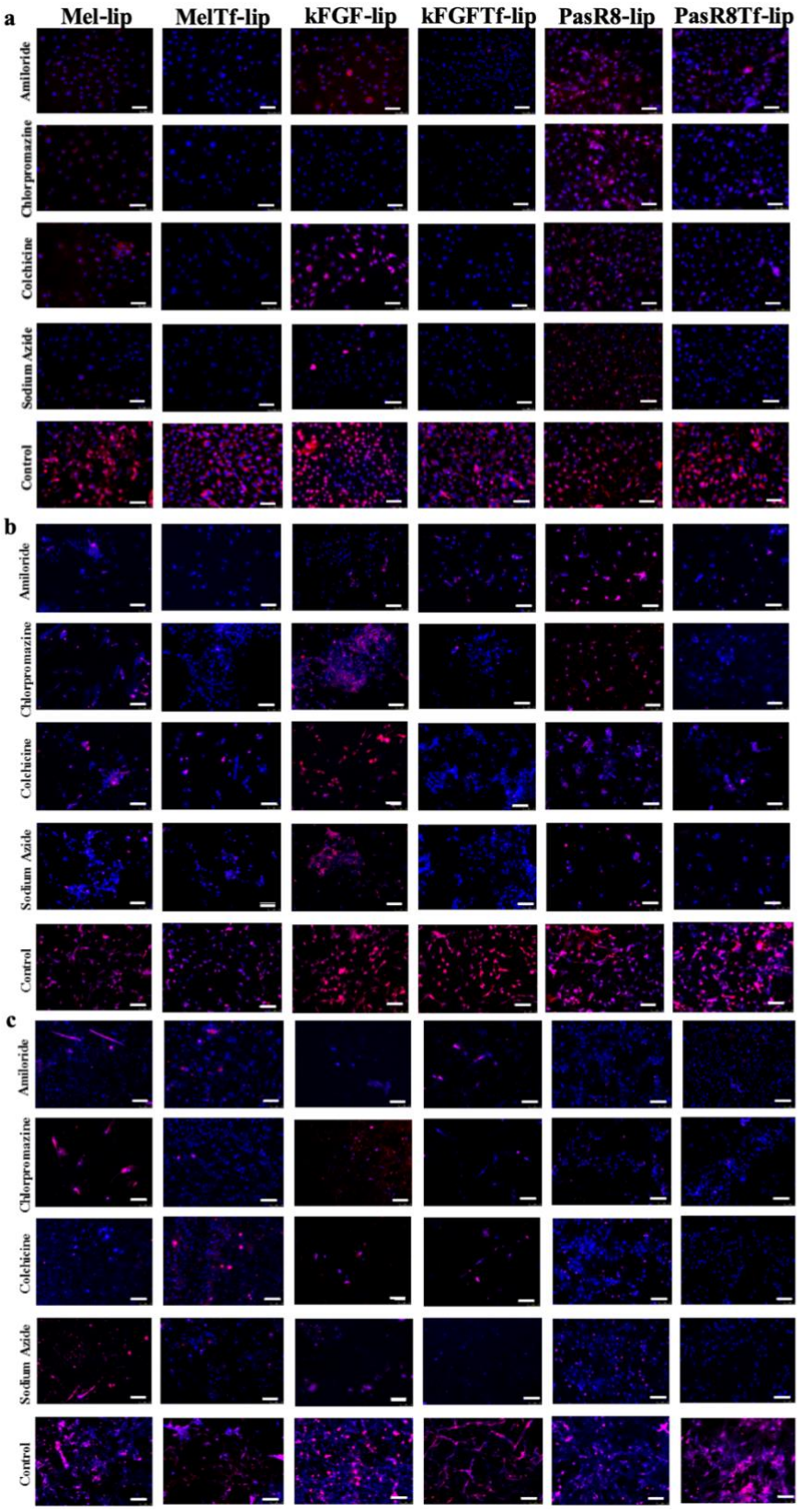
a
Mel-lip
MelTf-lip
kFGF-lip
kFGFTf-lip
PasR8-lip
PasR8Tf-lip
Amiloride
Chlorpromazine
Colchicine
Sodium Azide
Control
b
Amiloride
Chlorpromazine
Colchicine
Sodium Azide
Control
c
Amiloride
Chlorpromazine
Colchicine
Sodium Azide
Control

Supplemental Figure 1. Fluorescence microscopy images indicating the effect on uptake of Mel-lip, MelTf-lip, kFGF-lip, kFGFTf-lip, PasR8-lip and PasR8Tf-liposomes after 4 h of incubation in bEnd.3 (a), primary astrocytes (b) and primary neuronal cells (c) pretreated with endocytosis inhibitors (amiloride, chlorpromazine, colchicine and sodium azide) (Scale bar depicts 100 μm).

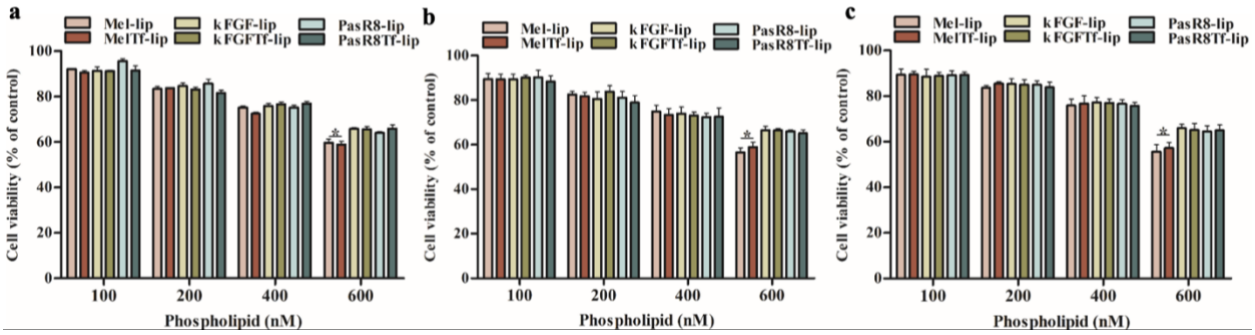

Supplemental Figure 2. β-galactosidase activity induced in bEnd.3 (a), primary astrocytes (b) and primary neuronal cells (c) after 48 h of treatment with Mel-lip, MelTf-lip, kFGF-lip, kFGFTf-lip, PasR8-lip and PasR8Tf -liposomes containing chitosan-pβgal complexes as determined by βgal assay kit. Data are expressed as mean ± SD (n=4). Statistically significant ($p<0.05$) differences are shown as (*) with control, (#) with Lipofectamine 3000 and (†) with Mel-lip, kFGF-lip and PasR8-liposomes.

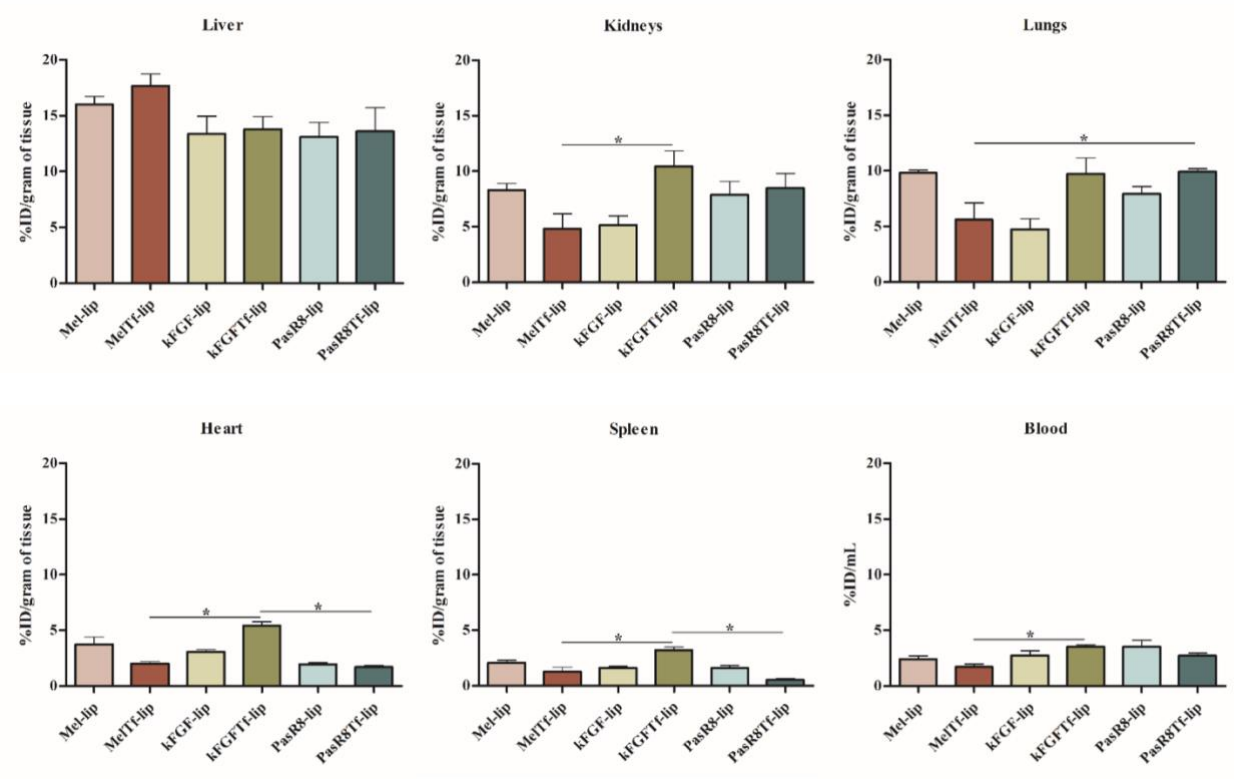

Supplemental Figure 3. *In vivo* biodistribution of Mel-lip, MelTf-lip, kFGF-, kFGFTf-, PasR8- and PasR8Tf-liposomes in liver, kidneys, heart, lungs, spleen and blood of CB57BL/6J mice after 24 h of liposomal administration. Data are expressed as mean ± SE (n=6). Statistically significant ($p<0.05$) differences are shown as (*).

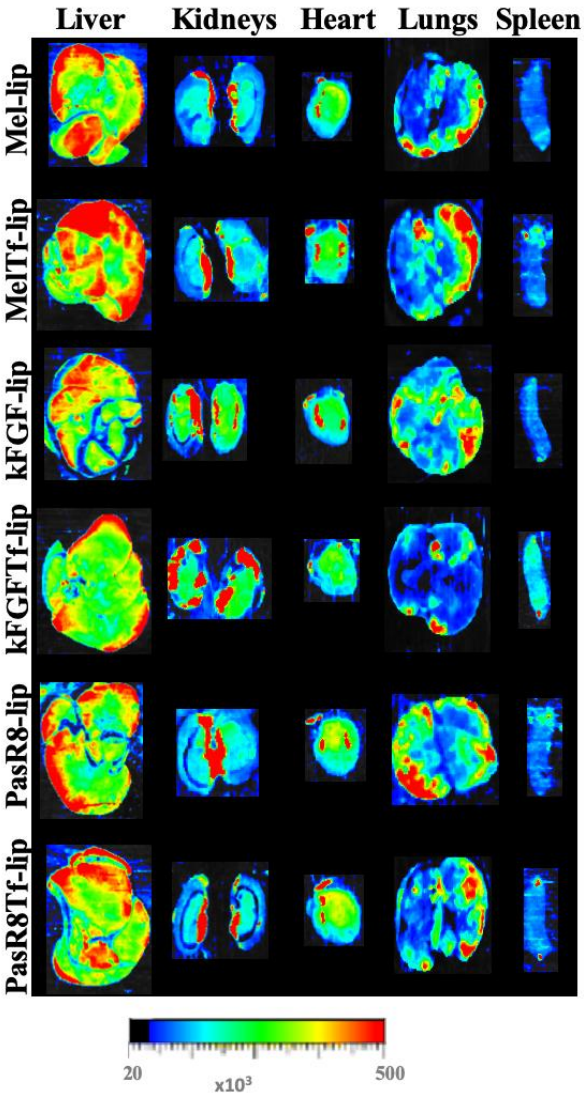

Supplemental Figure 4. Near-Infrared (NIR) imaging of relative fluorescence intensity in liver, kidneys, heart, lungs and spleen from C57BL/6J mice 24 h after administration of Mel-lip, MelTf-lip, kFGF-lip, kFGFTf-lip, PasR8-lip and PasR8Tf-liposomes.